

The power of high-effort seismic acquisition: the Longview experiment

David C. Henley, Malcolm B. Bertram, Kevin W. Hall, Henry C. Bland, Eric V. Gallant and Gary F. Margrave

ABSTRACT

Recent attempts have been made to reduce the “effort” involved in acquiring seismic data for exploration and development purposes by reducing the density of shots and receivers on the surface to that required only for properly imaging anticipated geological features with adequate lateral resolution. We show here, however, that there can be considerable benefits to actually increasing the acquisition density, particularly that of receivers. We recently conducted a carefully performed 1 km long 2D seismic survey east of Longview, Alberta using single geophones planted at 2.5 m intervals, with a mini-vibrator source applied at 5 m intervals. Using those data, we show that the fine spatial sampling enables not only superior coherent noise attenuation, but also significantly improves not only lateral resolution, but also vertical bandwidth, an unexpected result.

INTRODUCTION

In seismic exploration, there is always a trade-off between the quality of the seismic data acquired and the resources and “effort” committed to obtaining the data. For most routine seismic surveying, the acquisition geometry is designed to sample the anticipated subsurface features without spatially aliasing their structure, and to provide some amount of noise attenuation, while still allowing acceptable daily production rates. Noise attenuation has generally been provided by geophone arrays whose antenna pattern selectively admits mostly vertically-travelling reflection wavefronts, rather than the non-vertical wavefronts of coherent noise. Recent equipment advances, however, allow us to record individual geophones in sufficient numbers that we can eliminate arrays and reduce receiver station intervals dramatically. Doing this allows us to accomplish two objectives: the lateral resolution of a survey can be greatly improved, and we can use various processing tools for multi-channel noise attenuation. An earlier example of single phone acquisition relative to arrays is discussed for multi-component acquisition by Hoffe, et al. (2002).

While we describe the close-spaced, single geophone recording technique as “high effort”, the actual number of geophones per survey does not necessarily increase from that used in a conventional survey. What does increase is the number of phone/cable connections that must be made and broken during layout and pickup of the survey, as well as the density of source stations, since we typically shoot every other station, at the reduced station interval.

There are three objectives for our proposed technique: improved lateral resolution of reflection events; increased stack fold for higher S/N; and proper spatial sampling, not only of reflection features, but of all coherent noises, so that these noises can be effectively attenuated using multi-channel processes.

THE EXPERIMENT

Acquisition

In August 2006, several members of CREWES, as well as staff from the department of Geology and Geophysics, conducted a small seismic survey on a 1 km portion of a section line road intersecting secondary road 543 east of the town of Longview, Alberta. The experiment was intended as a shakedown test of the University's new seismic acquisition system (Bertram, et al., 2005) prior to the 2006 department field school, as well as a test of the "high-effort" method for high resolution surveys. Because of promising results from an earlier experiment using 5 m geophone spacing, the new survey was designed for 2.5 m spacing. The spread was 937.5 m in length, with 376 single geophone stations. For this survey, shots were spaced every 5 m along this line, which was shot from one end to the other without moving any portion of the spread. The source was the University's new mini-vibrator, emitting 4 sweeps per shot location, each sweep being 8 seconds, 10-200 Hz. Listening time was 10 seconds, and the data were saved, then diversity-stacked and correlated in the field for quality control.

Processing strategy

Creating data sets with coarser station spacing

The strategy for exploring the possible benefits of high effort seismic techniques was to first process the complete data set, taking every possible advantage of the short receiver interval to detect and remove noise, and to determine statics and velocities from the complete data set. Next, we created four other complete data sets by using all of the same original shot gathers, but decimating the receiver stations to simulate shot gathers with receiver intervals of 5 m, 10 m, 20 m, and 40 m. The decimation was done by applying appropriate trace mixing to the input gathers before decimation, to simulate using the original geophones in arrays, just as would typically be done in the field to attenuate non-vertically travelling wavefronts. We mixed 3 traces to increase to 5 m spacing, 5 traces to increase to 10 m spacing, etc. For these artificial data sets, although we used all the shot gathers, we effectively decimated the shot spacing as well, hence decimating the CDP interval and re-binning the traces. The effect of this is to create shot arrays with the array centres at the new, coarser shot interval. This means that all the traces of the original survey were used in creating each decimated data set, and that the stack fold at each decimated CDP was the same as the stack fold of the corresponding CDP in the original data set. Thus each decimated data set actually has higher fold than a data set acquired using a sparser, more conventional source spacing with no source array.

Noise removal and deconvolution

The processing flow for each of the data sets was identical, except that no parameters obtained from a visual examination of a particular data set were used to help process any of the more coarsely sampled data sets. Processing parameters depending upon receiver and/or CDP interval were individually assigned for each data set, but all other parameters were fixed at the same values for all data sets. The shot gathers were first analysed for coherent noise. All visible noises were sequentially estimated and subtracted using radial trace filtering (Henley, 2003a). Single trace mode Gabor deconvolution was then applied to the shot gathers after noise attenuation., since examination of the data sets showed that

ensemble mode deconvolution was not warranted for these data (Henley, 2006). Single trace mode Gabor deconvolution was also applied in the radial trace domain to all the gathers in each data set to remove the residual air blast, reduce short period multiples, and equalize reflection strength over angle (Henley, 2003).

Moveout velocity and statics

NMO Velocity analysis and statics derivation were the only two processing functions that were performed only on the 2.5 m data set and shared with the other sets, in the interest of providing comparable stack and migrated images in which the simulated receiver array geometry would be the only significant difference between the data sets.

Moveout analysis was performed on the shot gather displays of the 2.5 m data set, and the stacking velocities determined from these data were used for all the other data sets as well. Likewise, a horizon was picked on the brute stack of the 2.5 m data set as a guide for a maximum stack power residual statics program. The statics derived from the 2.5 m data set (with their superior statistics) were subsequently used for all the other data sets, as well. Since the statics were quite small (no static exceeded 5 ms), their application had relatively little effect on any of the stacks, except to slightly improve event bandwidth and continuity. Receiver statics for the simulated receiver arrays were assumed to be the statics of the individual 2.5 m receivers at the centres of the arrays. Statics for the individual phones in an array were *not* applied before array-forming, since these values would not be accessible to conventional surveys with hard-wired geophone arrays. Hence, unresolved inter-array geophone statics may have contributed to bandlimiting of the more coarsely sampled data sets. Shot statics for the original shot stations in the simulated shot arrays *were* applied, however, since the effective shot arrays were actually formed only at the CDP stacking stage.

Stacking, migration, and display

Each data set was CDP stacked with the common velocity function using the newly decimated CDP bins created for each data set. In order to create displays with comparable appearance, the four decimated raw stacks were interpolated to the same trace density as the original 2.5 m stack before plotting with variable density. FX phase spectra were computed for each raw stack, at the original lateral resolution of each individual stack, in order to identify the highest coherent frequency for each stack, and hence to guide the selection of migration parameters. These parameters were determined for each data set individually, so that the migration algorithm did not attempt to migrate aliased frequencies or dips. In order to honour the simulated spatial resolution of each data set, the raw stacks were migrated with a post-stack Kirchhoff algorithm, at their original simulated CDP resolution. Then, as with the raw stacks, the migrated sections were interpolated to the same final trace density before display

THE RESULTS

Input shot gathers

Figure 1 shows a typical shot gather from the 2.5 m data set. The spatial sampling has enabled the recording of the wavefield with very little aliasing of any reflection signal or coherent noise. On this gather, we can even see engine noise from the recording truck

generator travelling at air velocity from the left end of the spread, as well as some ground roll components travelling at much less than air velocity. The simulated 5 m version of the same shot gather is shown in Figure 2, where we can no longer see the generator noise, and the slower ground roll is seriously aliased in the center of the spread. Most other coherent noises are still well enough sampled to avoid aliasing. The 10 m version in Figure 3 begins to show aliasing even for some of the faster components of ground roll, in spite of the simulated 10 m wide geophone arrays. In fact, the arrays do not seem to enhance reflection energy significantly with respect to the noise, even though this is their sole purpose. Figure 4, with the 20 m simulated shot gather, shows aliasing for practically all the coherent noise except the first arrivals, and the reflections are still no more visible than on the other versions of the same shot. The 40 m simulated shot gather in Figure 5 is aliased for all coherent noise of any description, and reflections cannot be easily identified.

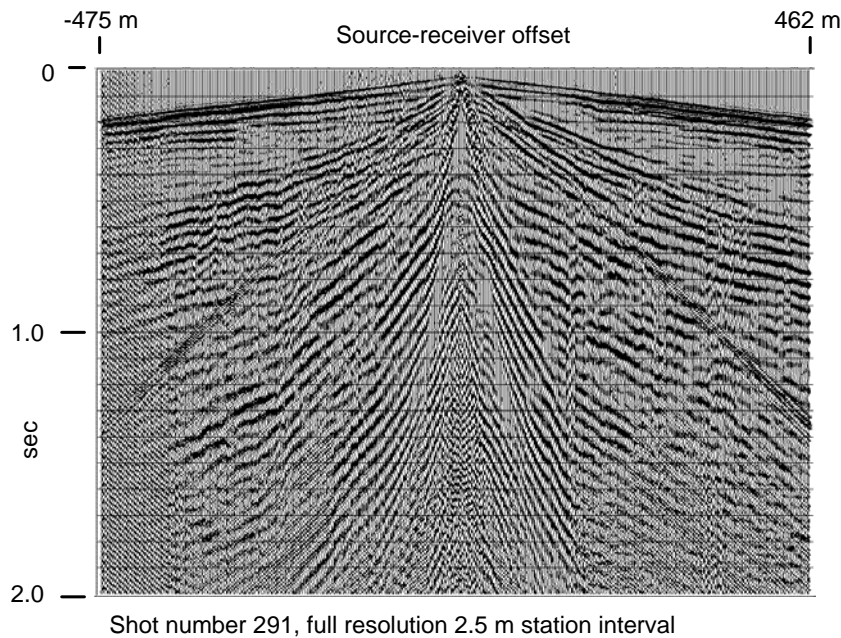


FIG. 1. A typical shot record from the Longview field survey with 2.5 m receiver spacing. Almost the whole wavefield is properly sampled.

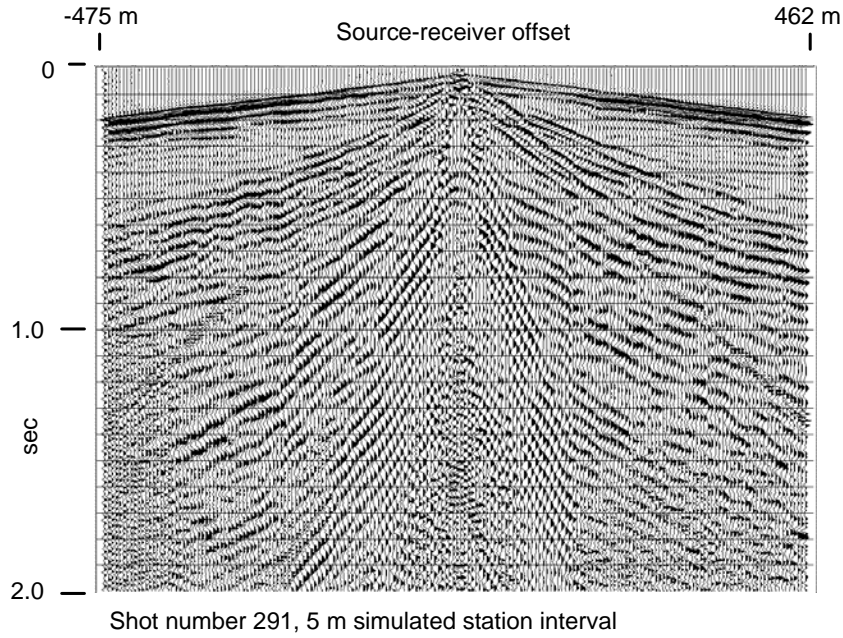


FIG. 2. Shot gather with simulated 5 m receiver spacing. Aliasing of some energy is evident on this gather.

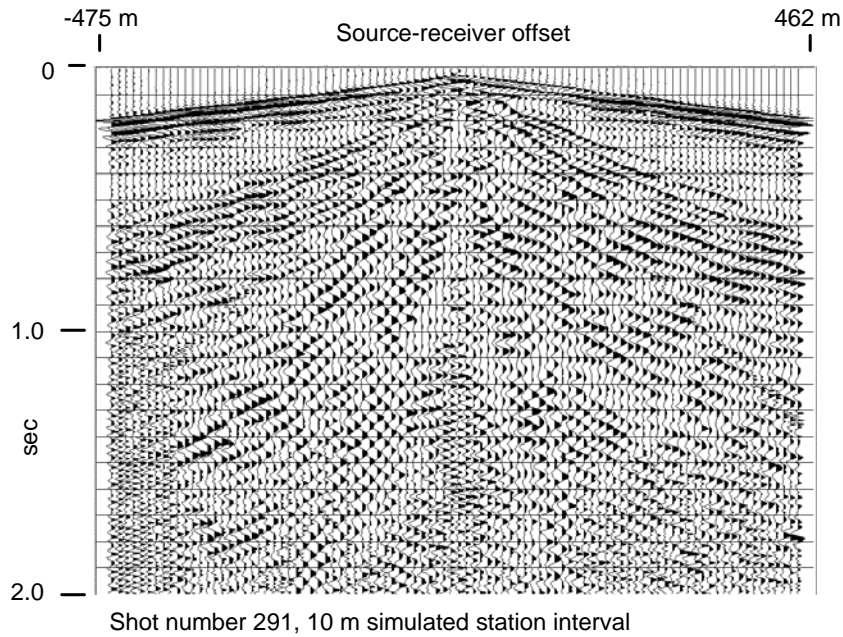


FIG. 3. Shot gather with 10 m simulated receiver spacing. Aliasing of events is now widespread.

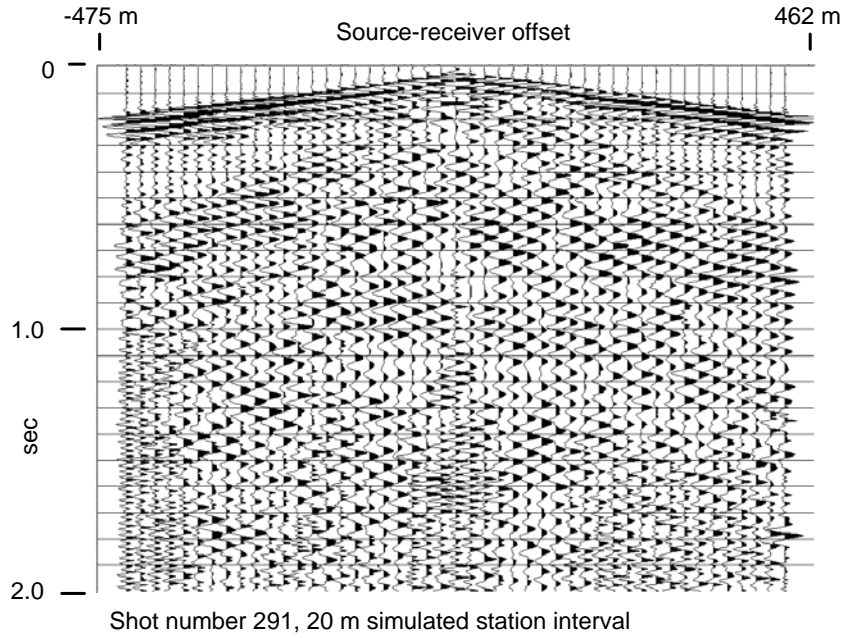


FIG. 4. Shot gather with simulated 20 m receiver interval. All noise events except the direct arrivals are aliased.

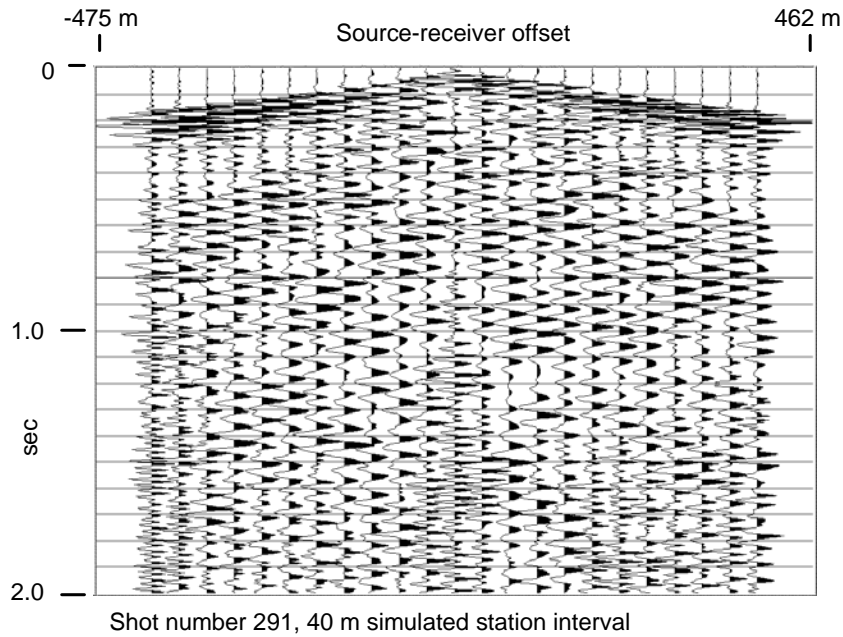


FIG. 5. Shot gather with 40 m simulated receiver interval. Even the direct arrival is aliased.

Noise removal

We illustrate coherent noise removal on the 2.5 m gather of Figure 1, but the procedure is the same for all other gathers. What declines as the receiver spacing increases is the ability to specifically detect noise coherence and apparent velocity, so that even though the same noise is present on all gathers (although attenuated by the simulated receiver arrays), it can't be detected, and no specific filter can be designed to remove it. Thus, a cascade of 7 radial trace filter passes can be designed and applied to the 2.5 m shot gathers, simply because at least that many coherent noise components can be characterized reliably. When the receiver spacing is increased to 40 m, however, no individual noises can be detected, and only a simple radial fan filter can be applied, leaving all the other noises undetected and relatively unattenuated, except for the modest effect of the simulated geophone arrays.

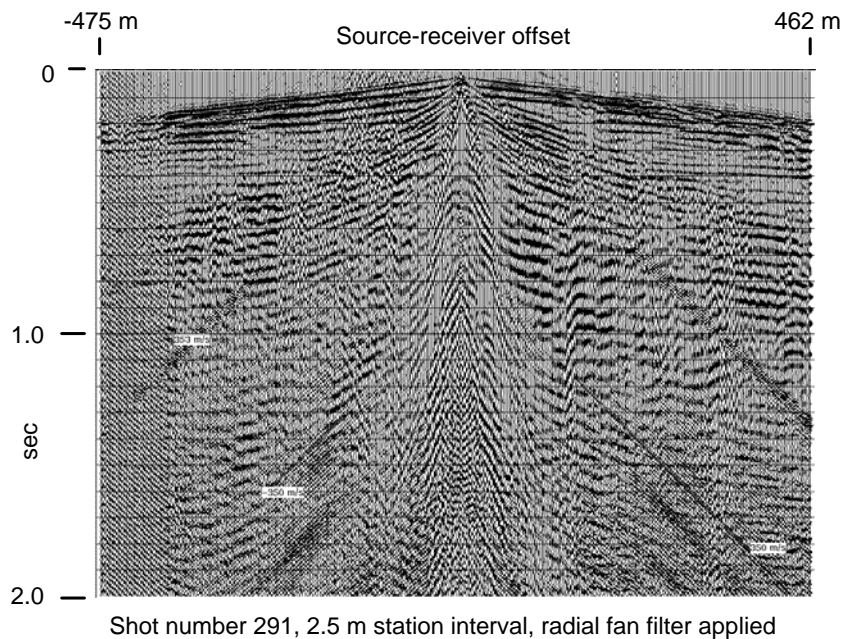


FIG. 6. 2.5 m shot gather after application of radial trace fan filter. Reflections are becoming visible, and various linear noises can be identified.

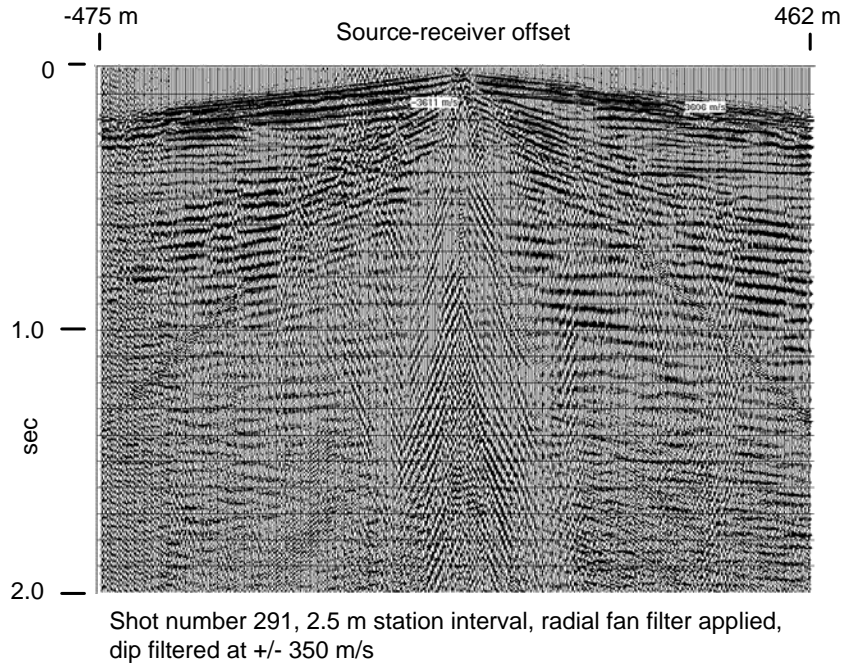


FIG. 7. 2.5 m shot gather after radial fan filter and a dip filter to remove air velocity noise.

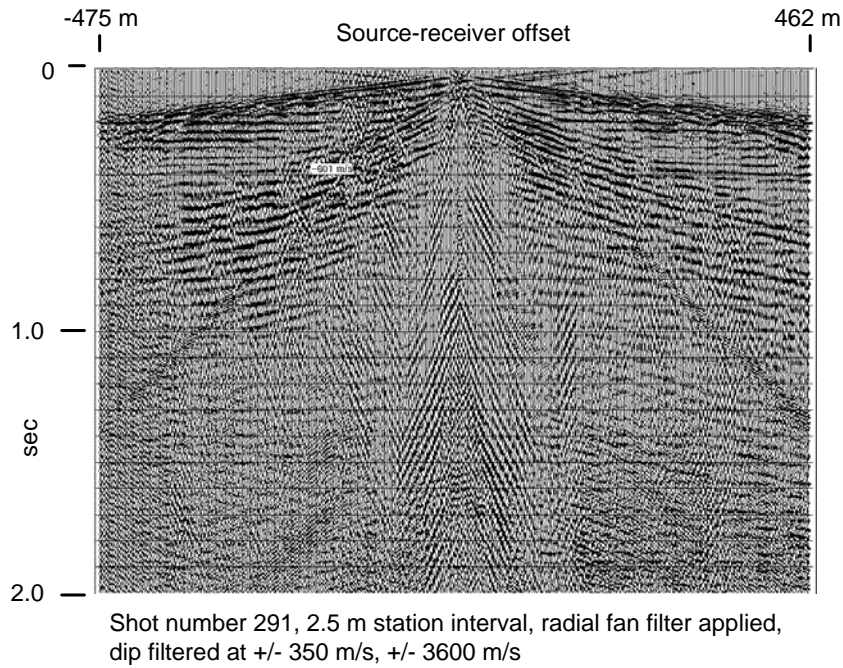


FIG. 8. 2.5 m shot after three stages of radial trace filtering.

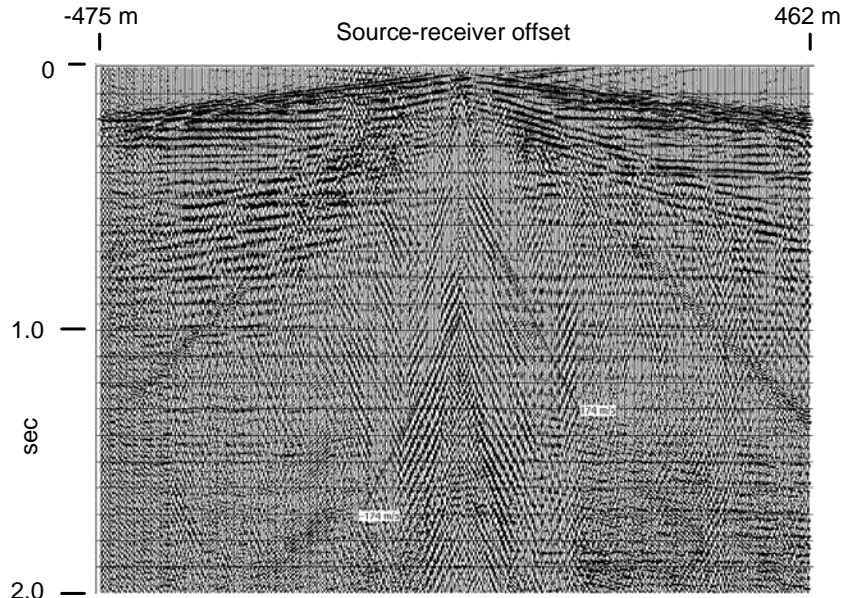


FIG. 9. 2.5 m shot after 4 stages of radial trace filtering.

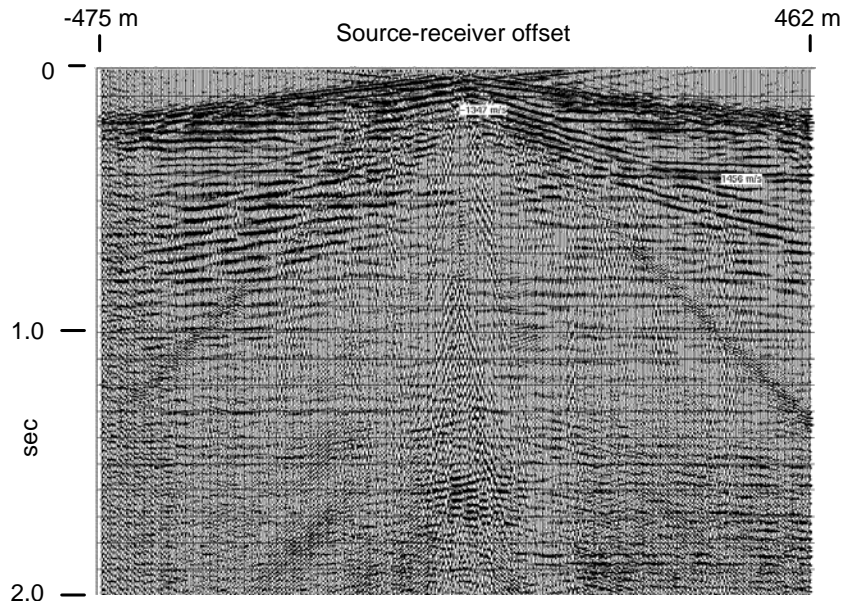


FIG. 10. 2.5 m shot after 5 stages of radial trace filtering.

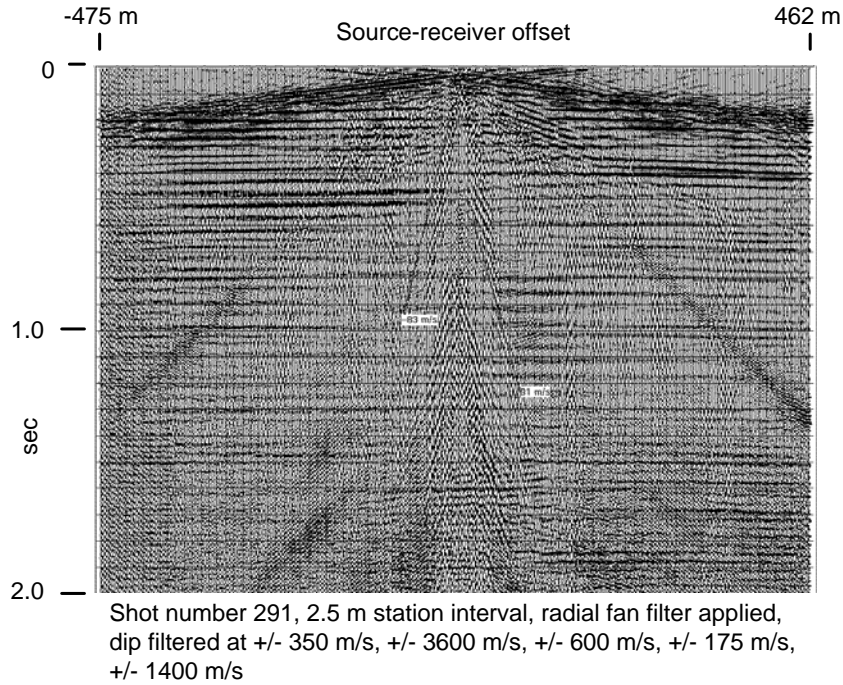


FIG. 11. 2.5 m shot after 6 stages of radial trace filtering.

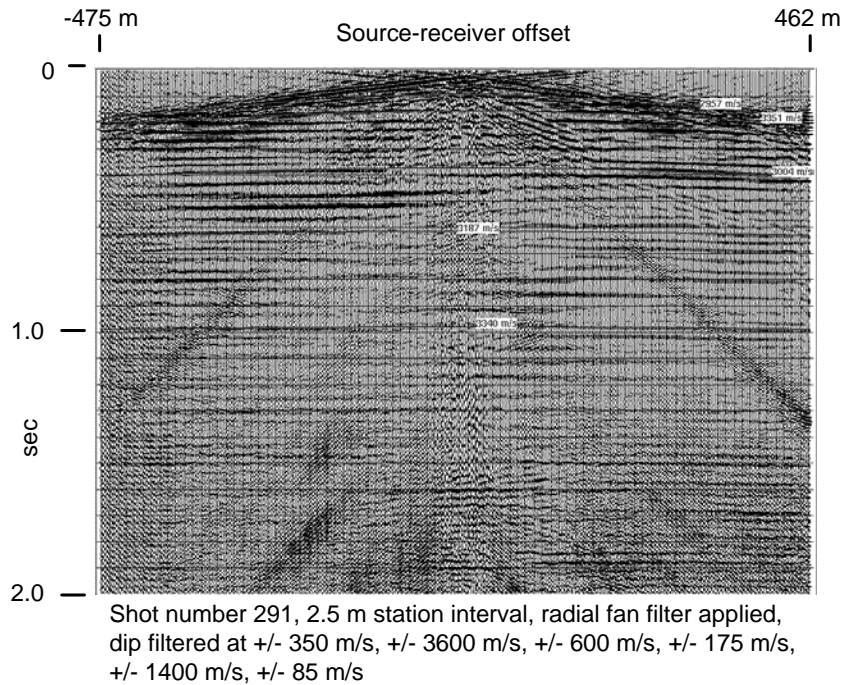


FIG. 12. 2.5 m shot after 7 stages of radial trace filtering.

Figure 6 shows the gather in Figure 1 after application of the radial trace fan filter. This filter estimates all linear noises that originate at the shot location and subtracts the estimate from the gather. Note the significant removal of first arrival energy and some of

the ground roll, and the increased visibility of reflections on the right side of the gather. Figure 7 shows the result of radial trace dip filter passes in which linear events of air velocity are estimated and subtracted. Linear noise with apparent velocity of ± 3600 m/s is removed next in Figure 8, and Figures 9, 10, 11, and 12 show subsequent removal of linear noises with velocities measured in the previous panel. The general diagnostic approach is to apply a fan filter, examine the result to identify any prominent remaining linear noise, apply a filter to estimate and subtract that noise, look for other remaining noises, subtract them, and so forth. After removing all these layers of noise, the reflections left on Figure 12 are greatly enhanced and can be analyzed for moveout velocity, as seen in the Figure.

The noise removal on all the reduced resolution data sets proceeds in exactly the same fashion, except that due to aliasing, fewer and fewer noises can be identified on the raw gathers. When the simulated receiver spacing is 20 m, only one coherent linear noise can be seen and removed after the initial fan filter; and on the 40 m data set, no noises can be identified.

Deconvolution

After coherent noise attenuation, the next processing step is deconvolution, to broaden the reflection signal spectrum and adjust the time-varying amplitudes of the traces. Figure 13 shows the 2.5 m shot gather after a pass of single trace mode Gabor deconvolution. We can still see some coherent noise residual on this gather, as well as some zones of reduced amplitude where noise has been subtracted. These anomalies all appear to be oriented toward the origin of the gather, so we transform to the radial trace domain and apply Gabor deconvolution in that domain to fix these problems, as well as to reduce possible interbed multiples. The result, for the 2.5 m shot, is shown in Figure 14. This gather has undergone a remarkable improvement from its original version in Figure 1, and it should be emphasized that most of this improvement is due to the noise analysis and processing enabled by the short receiver interval.

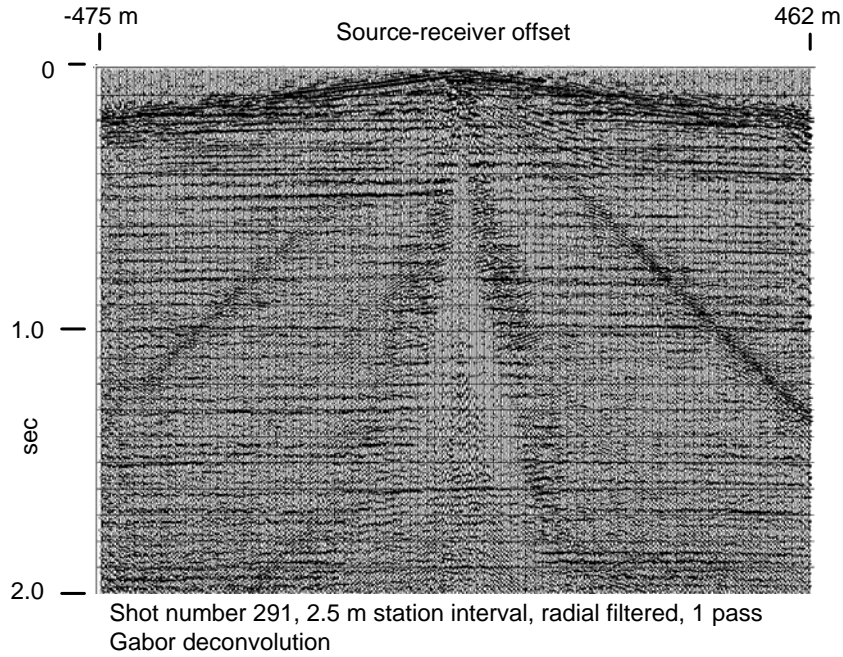


FIG. 13. 2.5 m shot after noise removal, Gabor deconvolution in the XT domain.

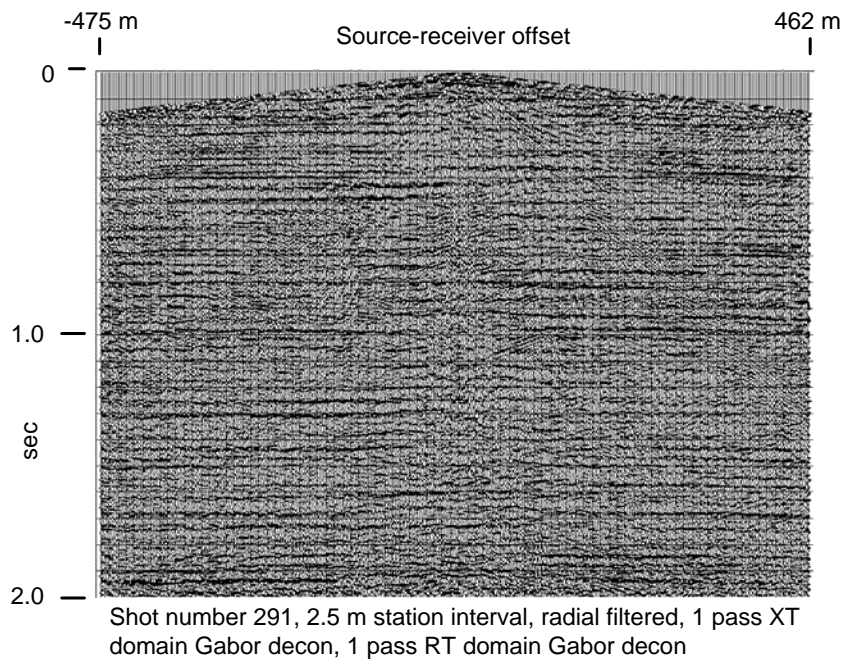


FIG. 14. 2.5 m shot after noise removal, Gabor deconvolution in the XT domain, and Gabor deconvolution in the RT domain.

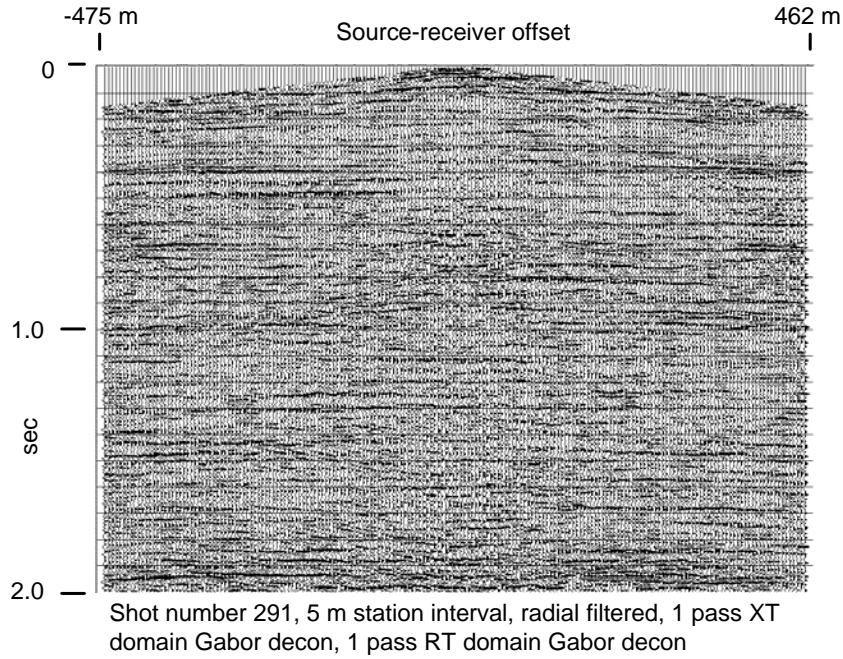


FIG. 15. 5 m shot after noise removal and Gabor deconvolution in both XT and RT domains.

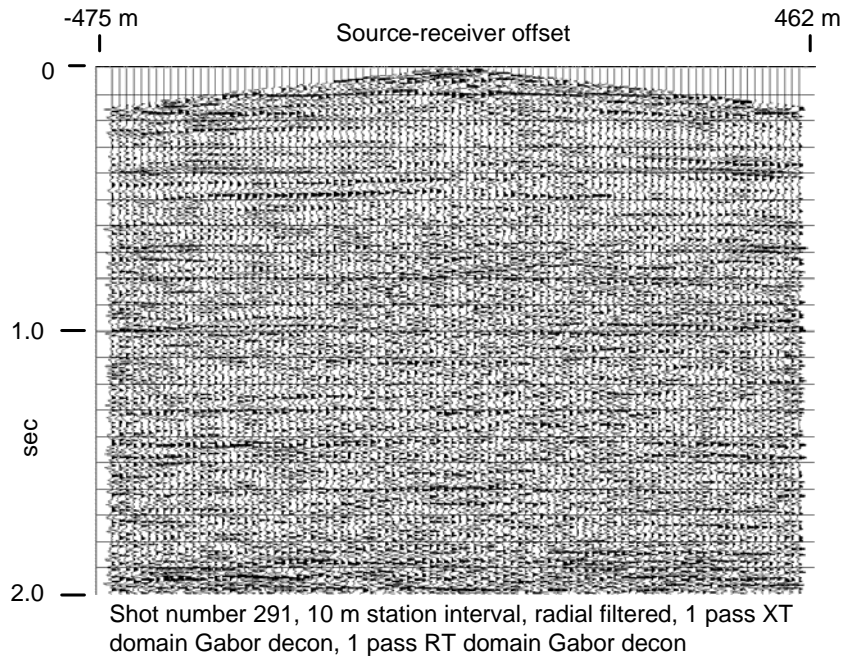


FIG. 16. 10 m shot after noise removal and Gabor deconvolution in both XT and RT domains.

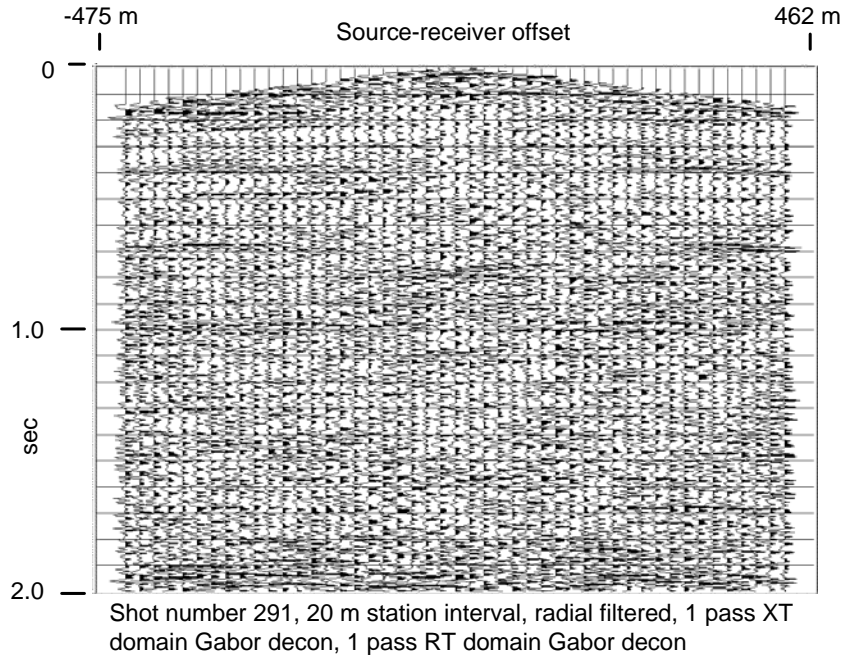


FIG. 17. 20 m shot after noise removal and Gabor deconvolution in both XT and RT domains.

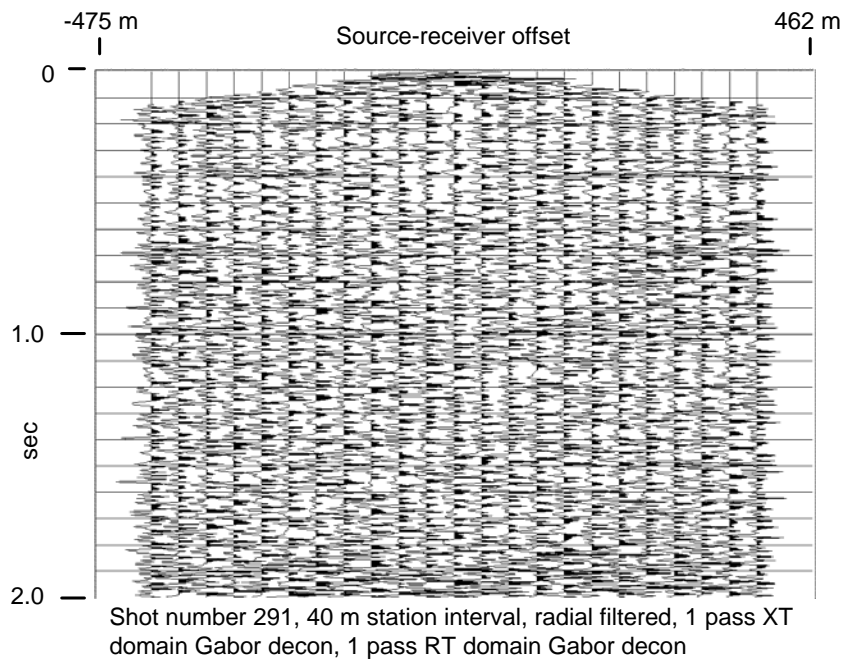


FIG. 18. 40 m shot after noise removal and Gabor deconvolution in both XT and RT domains.

After noise removal, the gathers of the other data sets were also deconvolved with Gabor deconvolution, first in the XT domain, then in the radial trace (RT) domain. The results are shown in Figures 15, 16, 17, and 18, for the 5 m, 10 m, 20 m, and 40 m data sets, respectively. These figures speak for themselves in terms of noise removal and improved signal coherence (or lack thereof). It is evident that much less reflection enhancement is possible as the receiver increment increases, and that the simple summation within receiver arrays does not adequately attenuate coherent noise compared to processing algorithms like radial trace filtering.

The stack

Shot gathers alone provide no definitive diagnostics for lateral resolution studies, so we applied NMO and statics and stacked all five data sets to yield the displays shown in Figures 19, 20, 21, 22, and 23. At first glance, the biggest differences seen in these stacks are in the apparent lateral resolution in the near surface—the reflections, on this scale, look similar on all the stacks. Nevertheless, we computed FX phase spectra for each of these stacks, as shown in Figures 24, 25, 26, 27, and 28. These show that the laterally coherent part of the spectrum is incrementally reduced for each reduction in the lateral resolution of the data set. This seems surprising until we recall that the more coarsely spaced gathers have more undetected residual coherent noise, which almost certainly limits the bandwidth of the reflection signal.

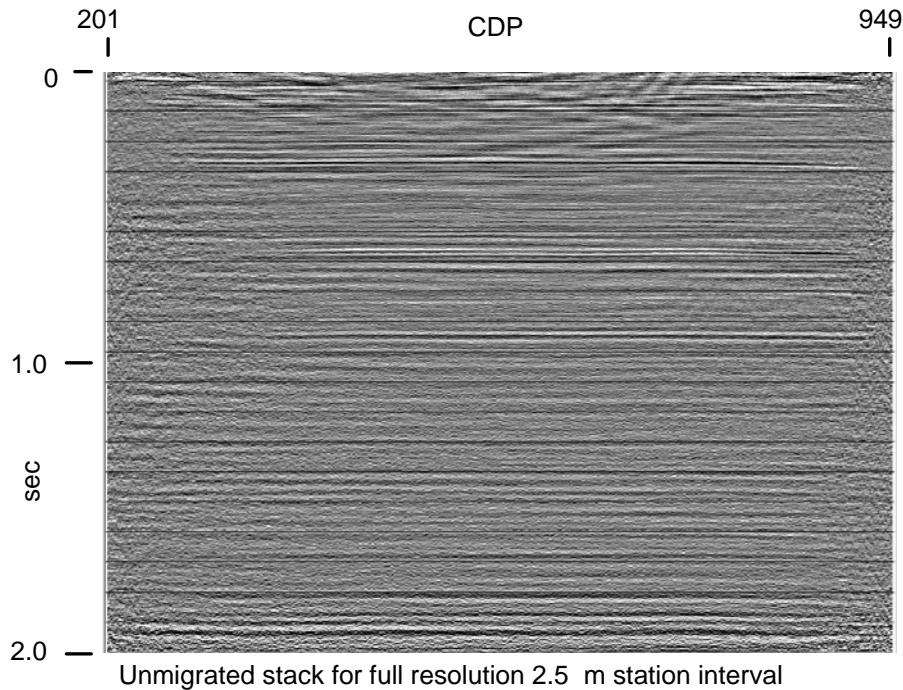


FIG. 19. Final unmigrated stack for 2.5 m data.

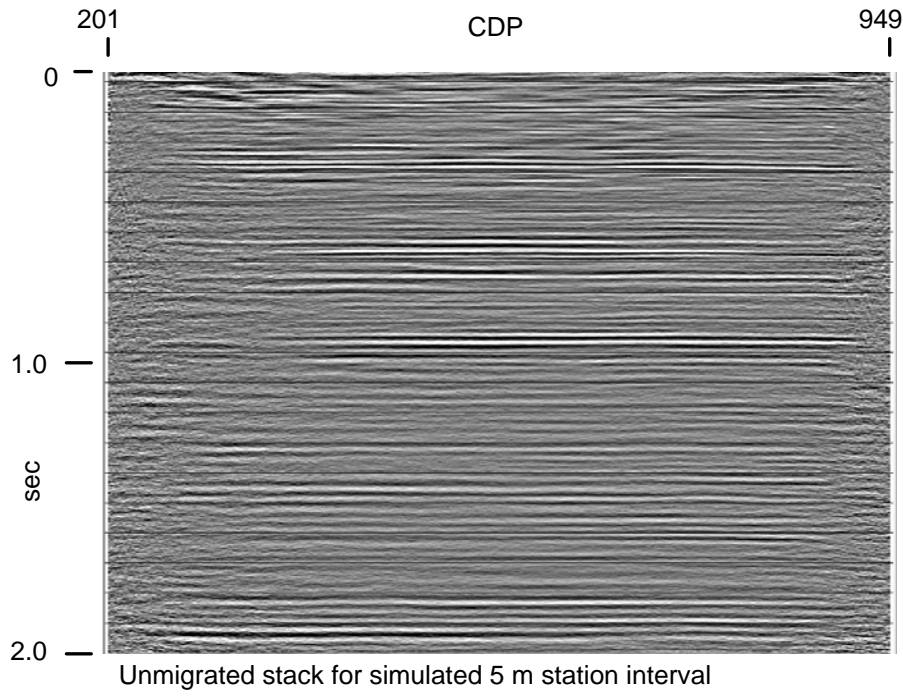


FIG. 20. Final unmigrated stack of 5 m data.

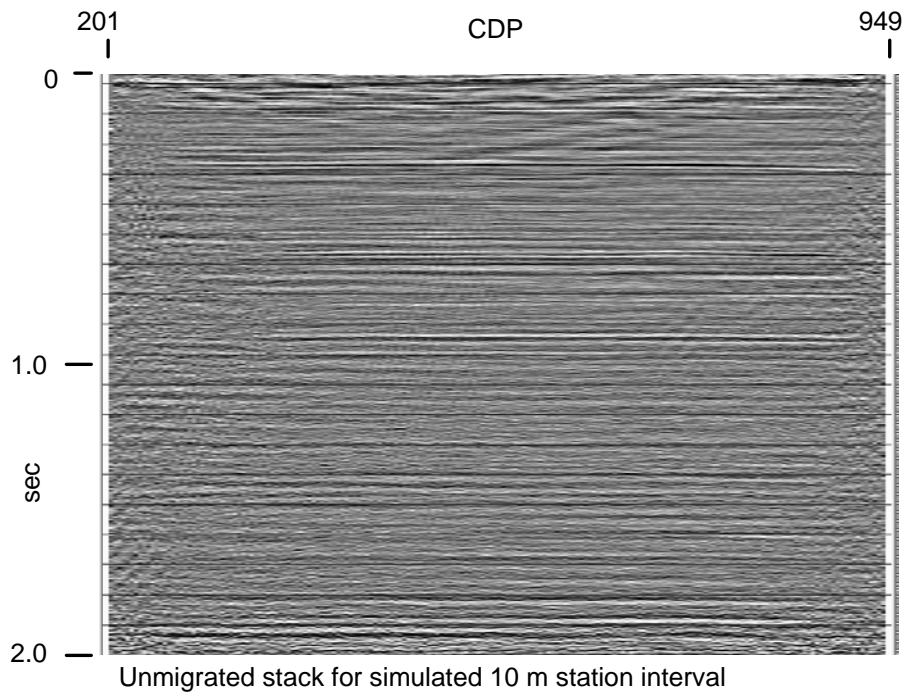


FIG. 21. Final unmigrated stack of 10 m data.

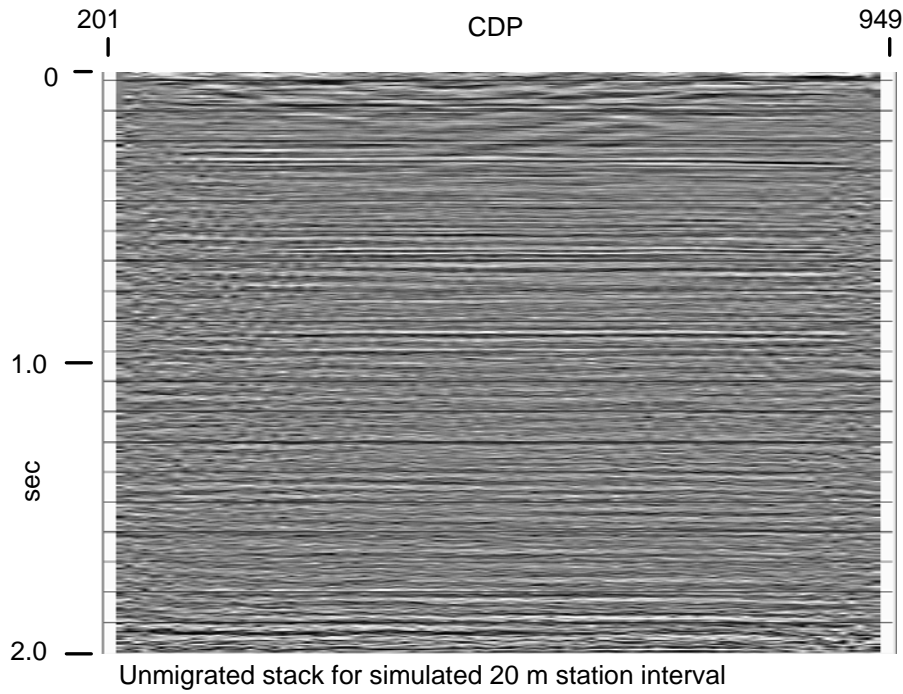


FIG. 22. Final unmigrated stack of 20 m data.

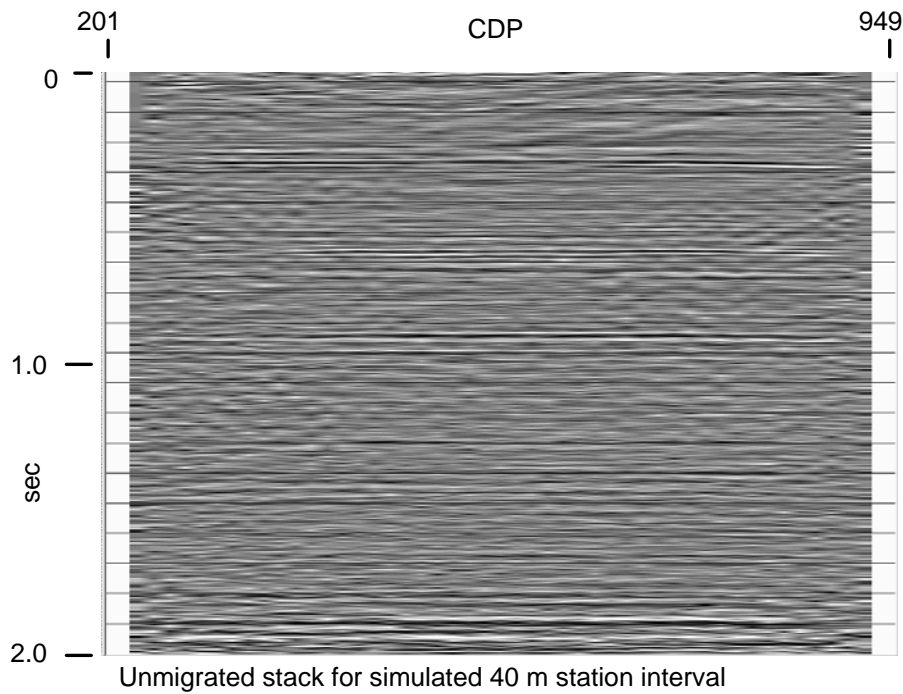


FIG. 23. Final unmigrated stack of 40 m data.

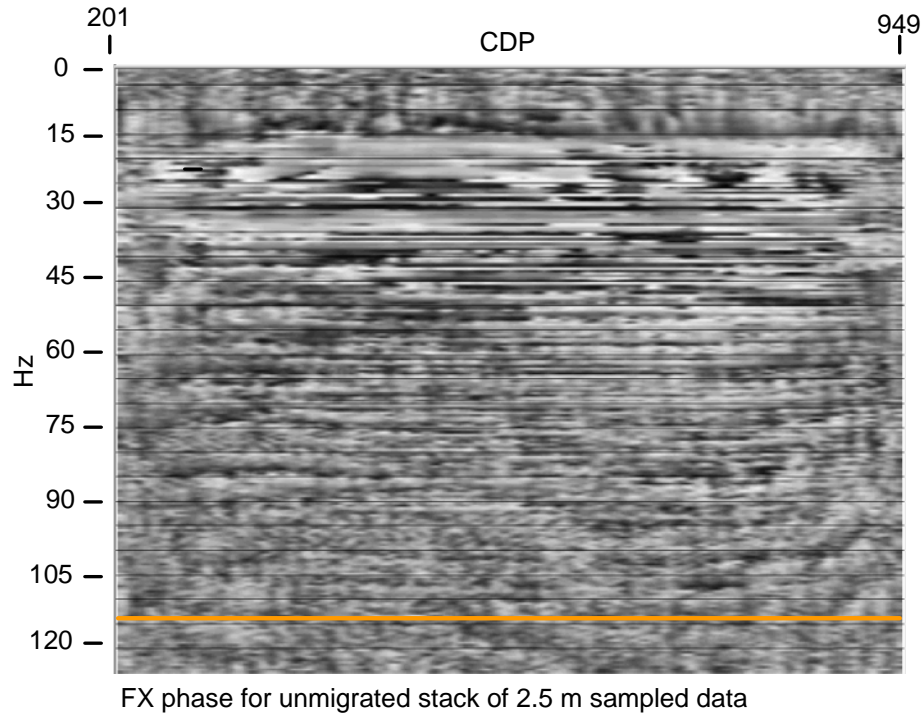


FIG. 24. FX phase spectrum of 2.5 m stack. Phase coherence visible to nearly 110 Hz.

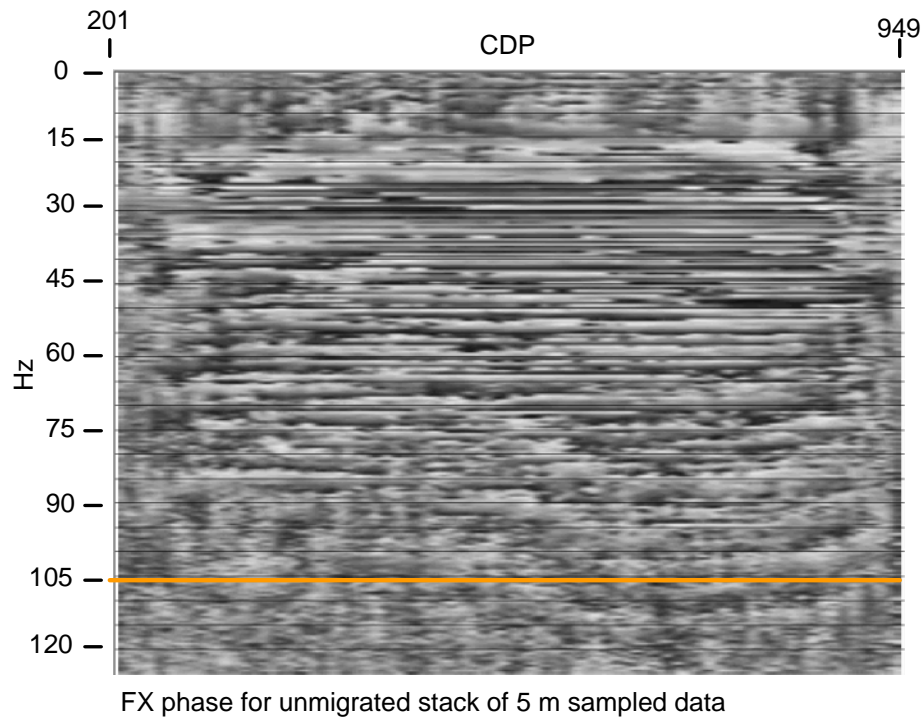


FIG. 25. FX phase spectrum for 5 m stack. Phase coherence extends to about 105 Hz.

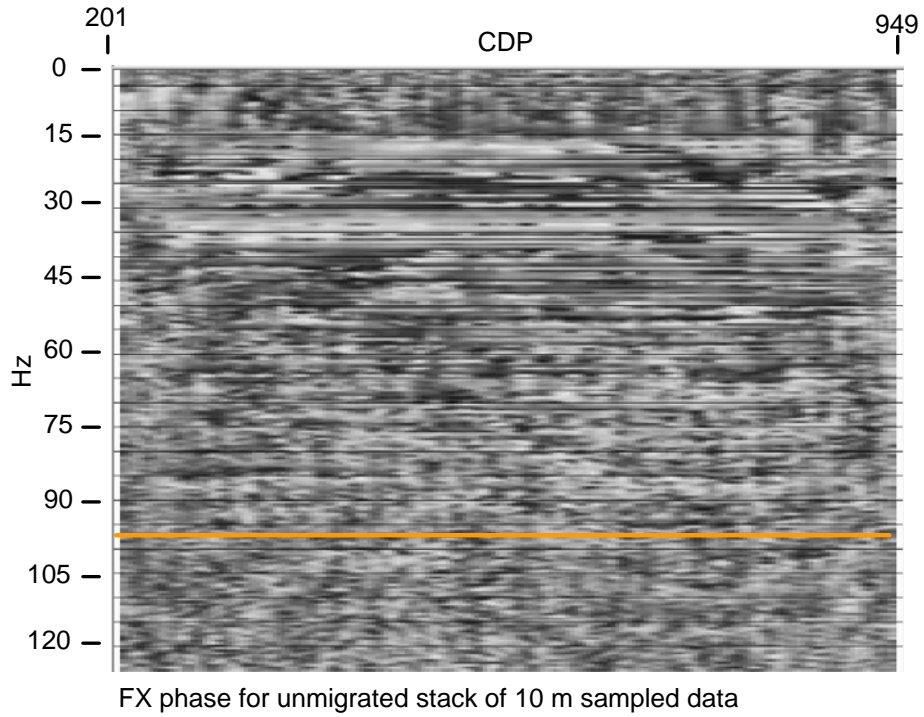


FIG. 26. FX phase spectrum for 10 m stack. Phase coherence extends to about 95 Hz.

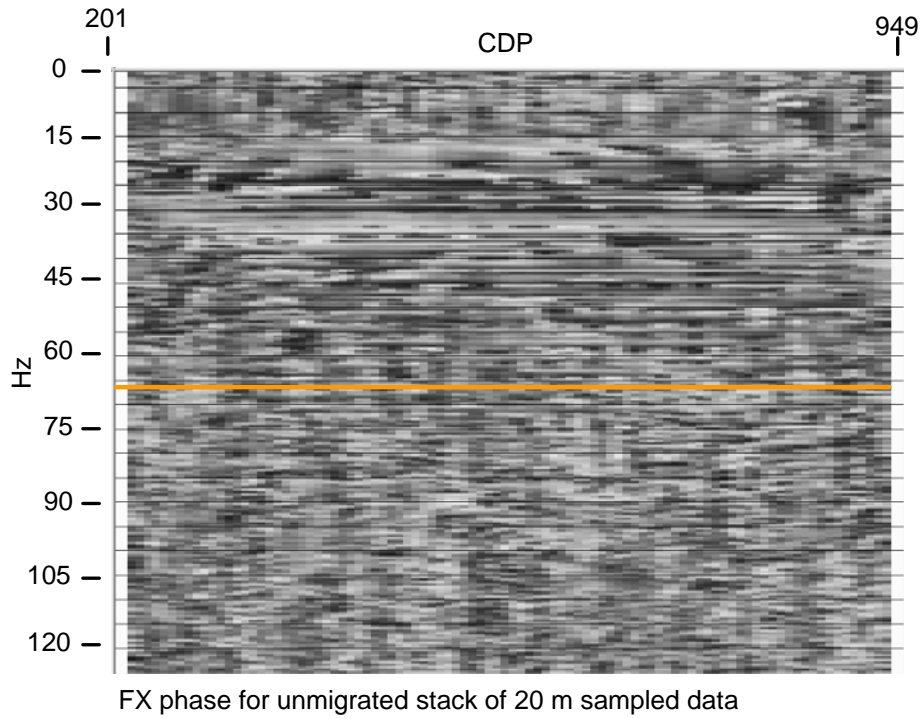


FIG. 27. FX phase spectrum for 20 m stack. Phase coherence extends to about 65 Hz.

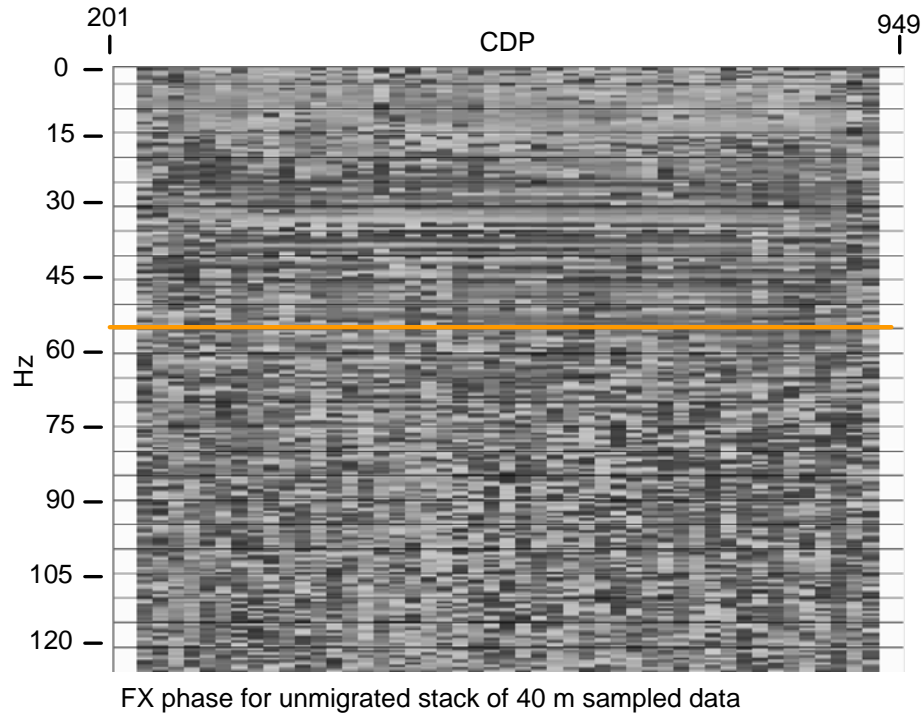


FIG. 28. FX phase spectrum for 40 m stack. Phase coherence extends to about 55 Hz.

The final images

The ultimate test of lateral (and vertical) resolution of any data set is to migrate the data and judge the resulting image for both lateral and vertical coherence and resolution. Starting with the raw stacks, and using the FX spectra as guides to the maximum frequency to migrate, the five data sets were migrated using a Kirchhoff post-stack algorithm and the same velocity function as was used for stacking. The resulting migrated stacks were then interpolated to the same trace density, to make comparable displays. To compare the images in more detail than the raw stacks, we selected four different zoom views of the output image in Figure 29 and show here each of the five data sets for each zoom view. Hence, Figures 30, 31, 32, 33, and 34 show zoom view 1 for the 2.5 m, 5 m, 10 m, 20 m, and 40 m data sets, respectively. Likewise, Figures 35, 36, 37, 38, and 39 show zoom view 2 for the same data sets; Figures 40, 41, 42, 43, and 44 show zoom view 3; and Figures 45, 46, 47, 48, and 49 show the fourth and final zoom view (also at a different plotting scale). Careful comparison of all these images convinces us that, indeed, the 2.5 m data set has the best lateral (and vertical) resolution and continuity at all levels, followed in order by the 5 m, 10 m, 20 m and 40 m data sets.

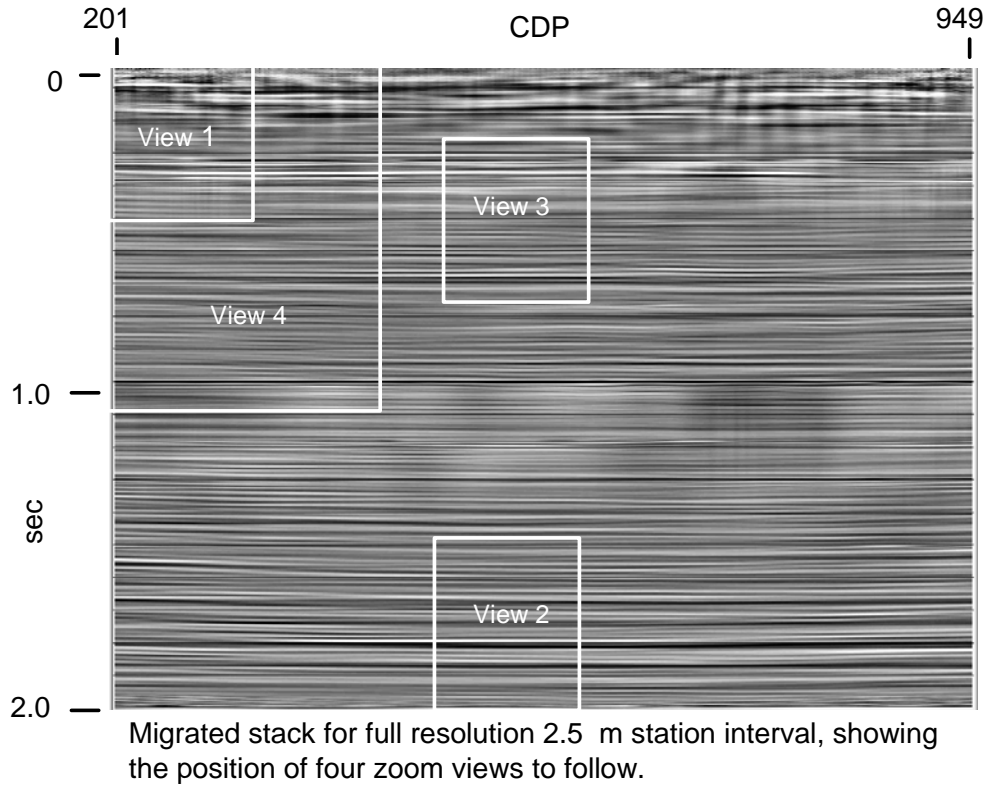


FIG. 29. Migrated stack for 2.5 m station interval. In order to compare the detail in this and the other migrated stacks, we examine each migrated stack in each of the four zoom windows shown above.

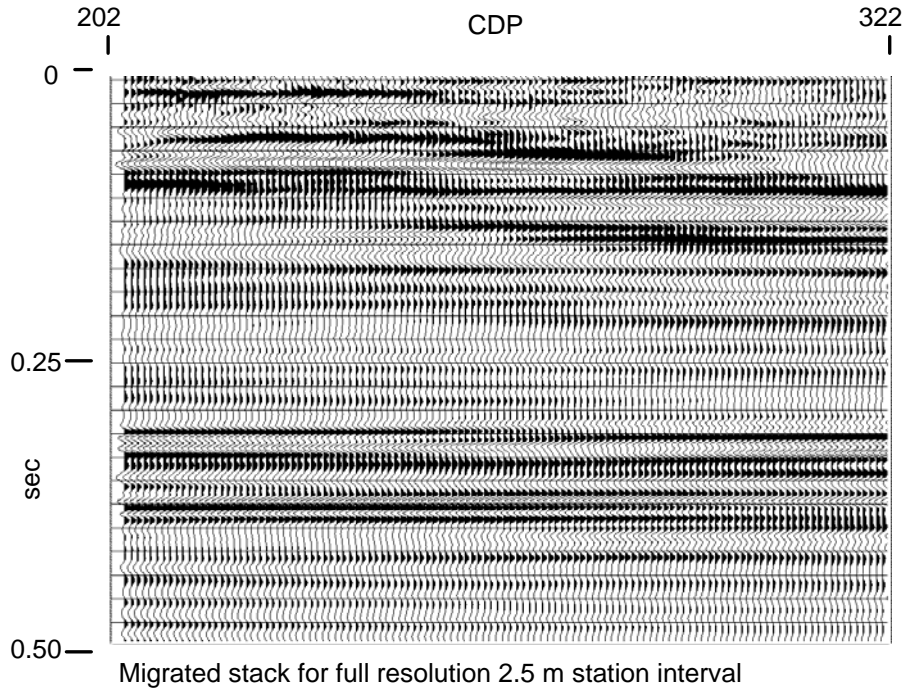


FIG. 30. Migrated stack image for the 2.5 m data set—view 1

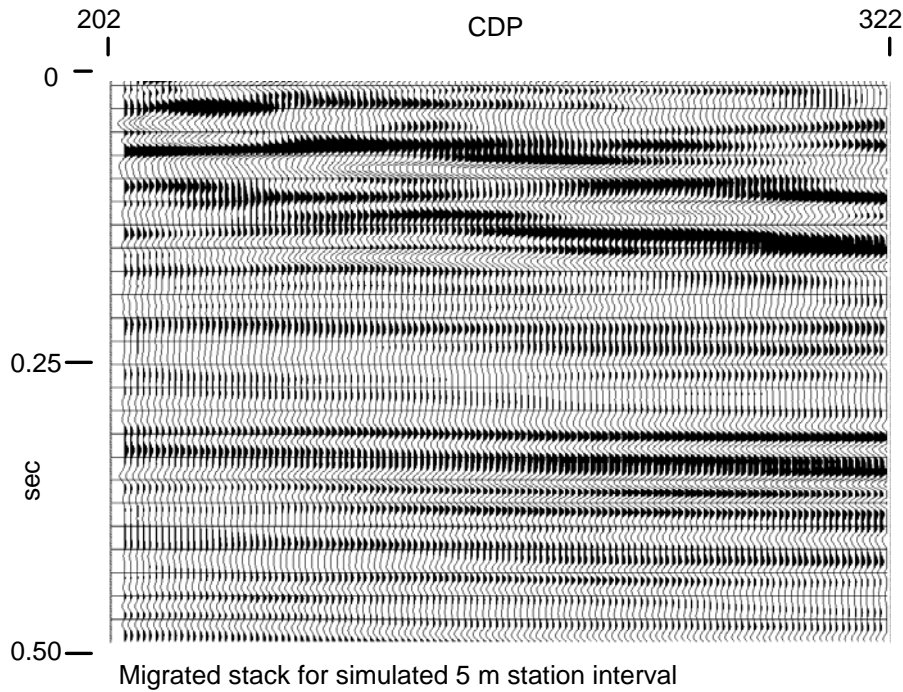


FIG. 31. Migrated stack image for the 5 m data set—view 1

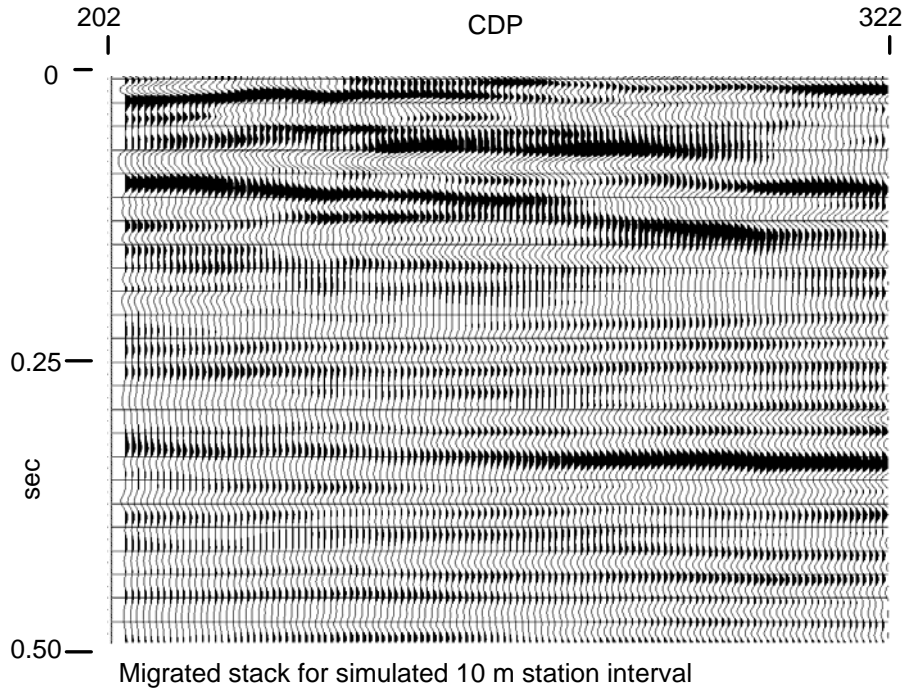


FIG. 32. Migrated stack image for the 10 m data set—view 1

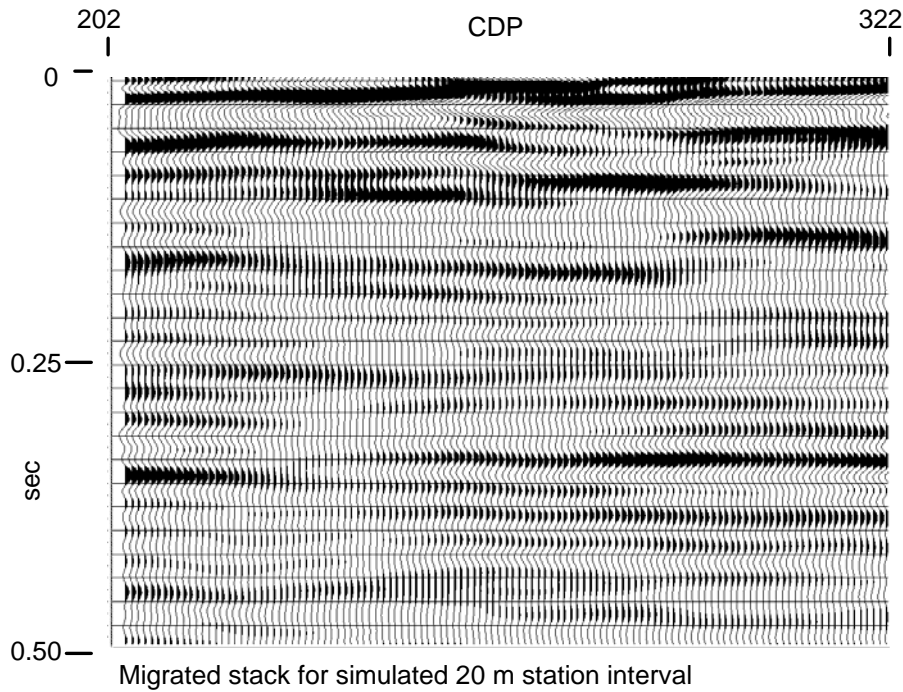


FIG. 33. Migrated stack image of 20 m data—view 1

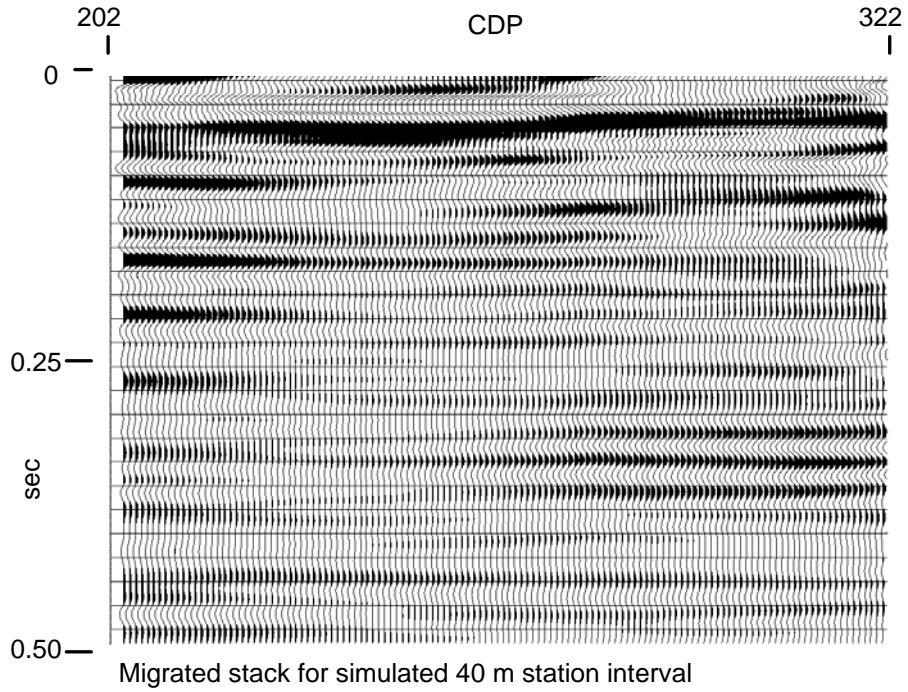


FIG. 34. Migrated stack image of the 40 m data set—view 1

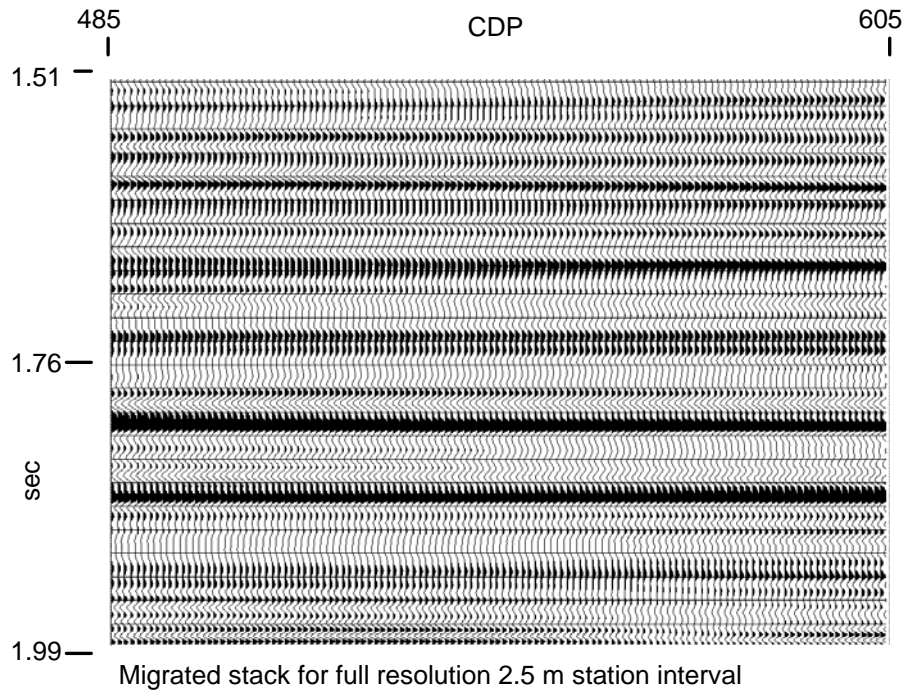


FIG. 35. Migrated stack image of 2.5 m data—view 2

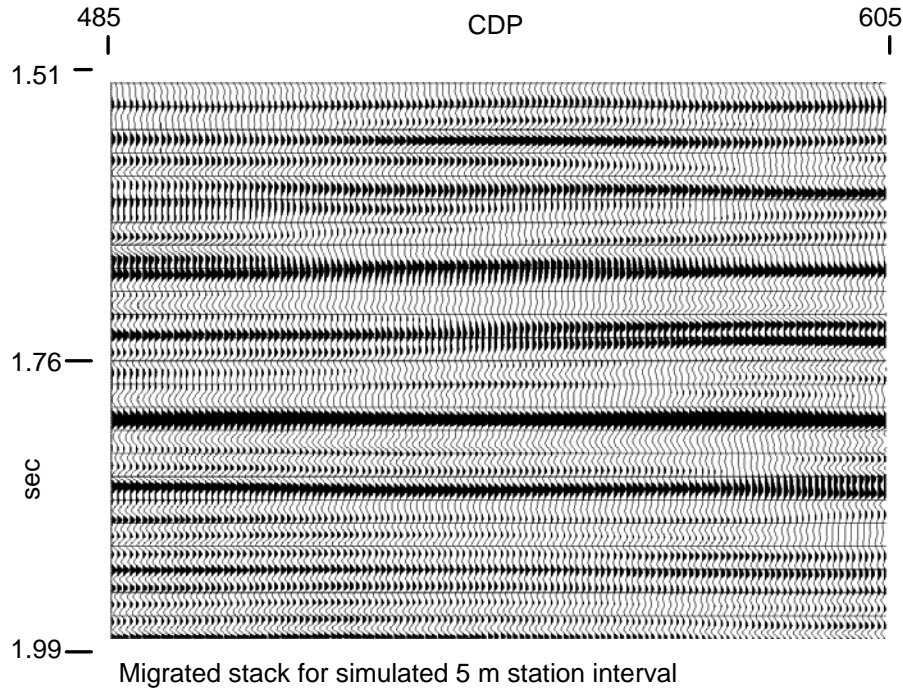


FIG. 36. Migrated stack image of 5 m data—view 2

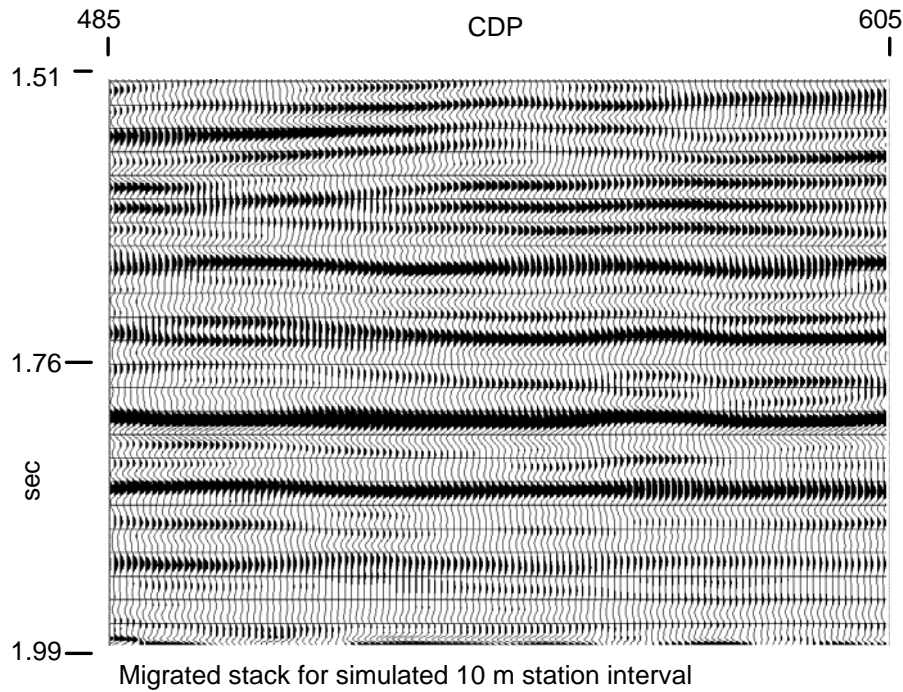


FIG. 37. Migrated stack image of 10 m data—view 2

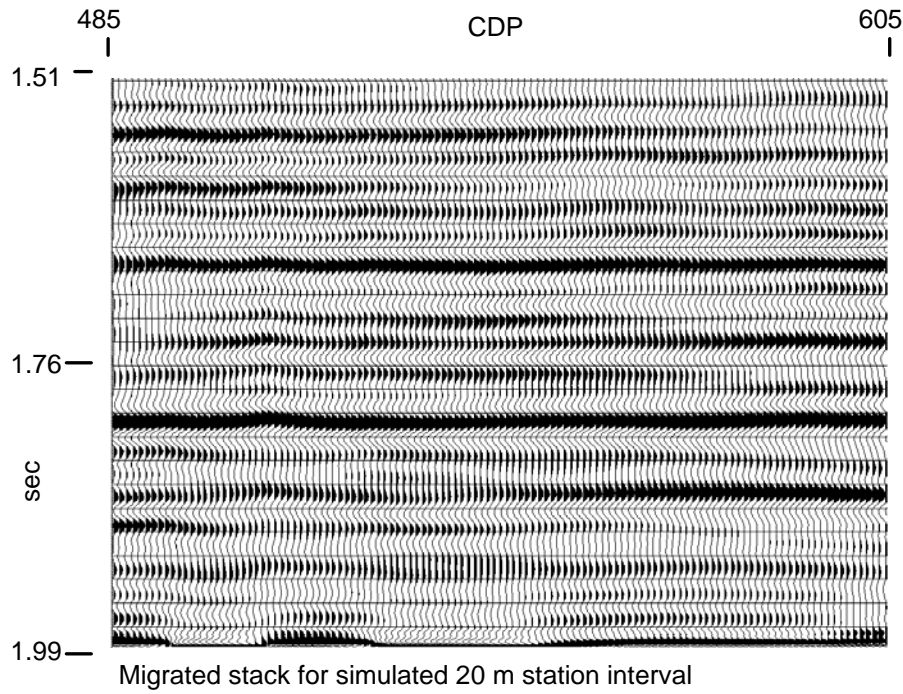


FIG. 38. Migrated stack image of 20 m data—view 2

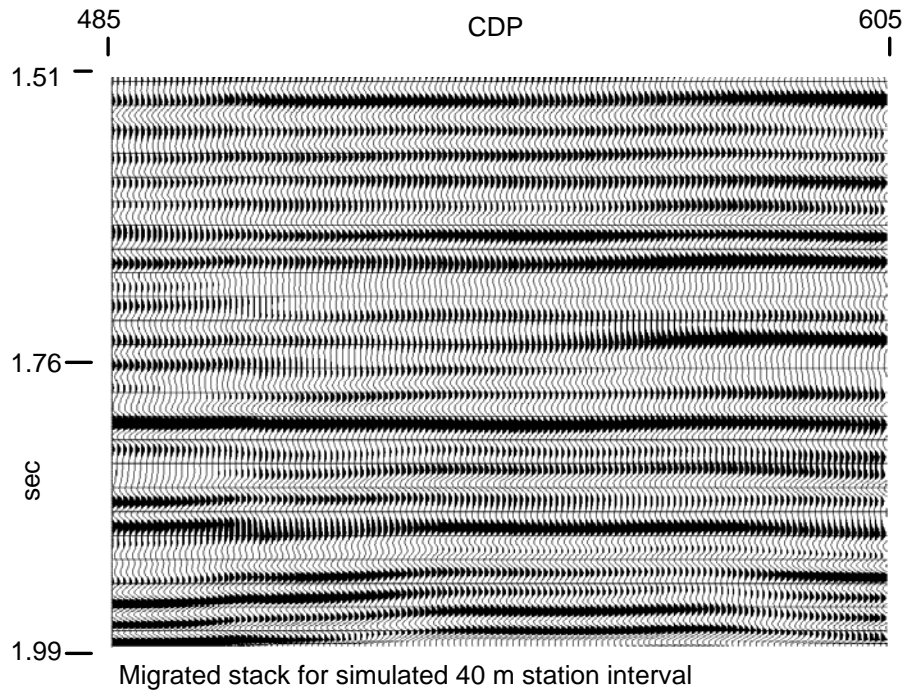


FIG. 39. Migrated stack image of 40 m data—view 2

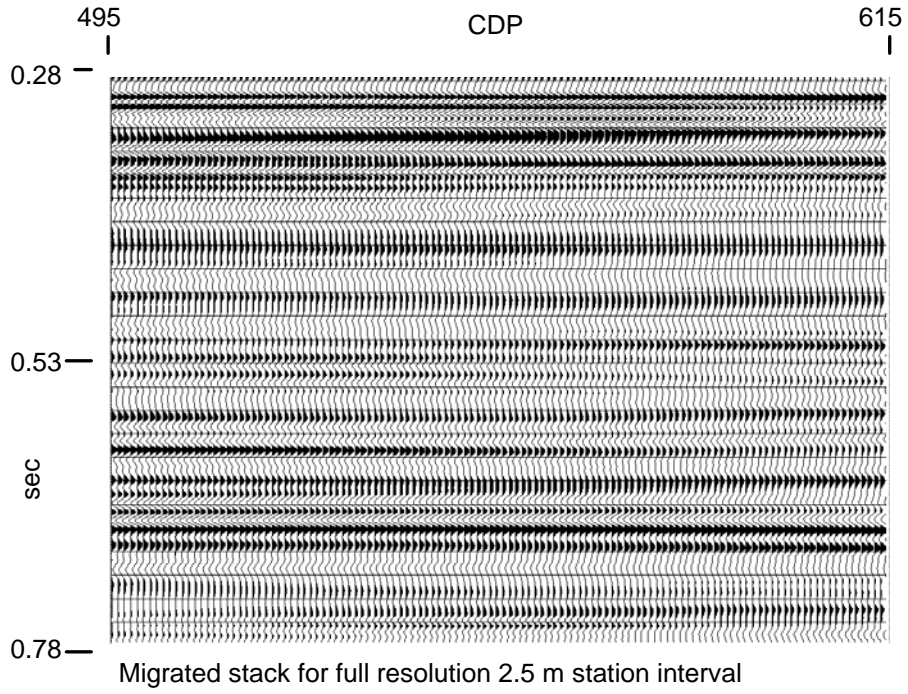


FIG. 40. Migrated stack image for 2.5 m data—view 3

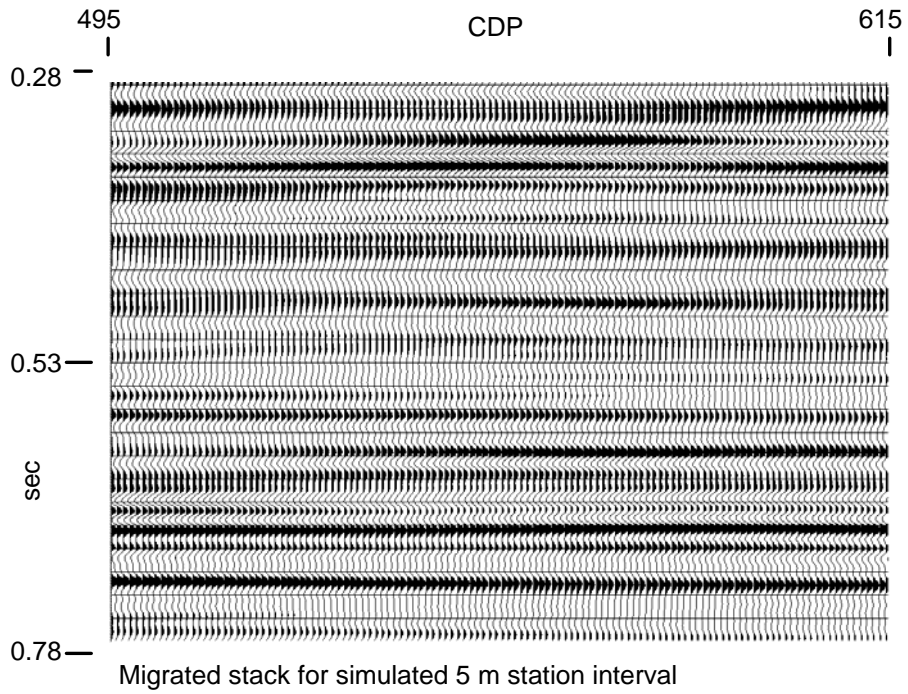


FIG. 41. Migrated stack image of 5 m data—view 3

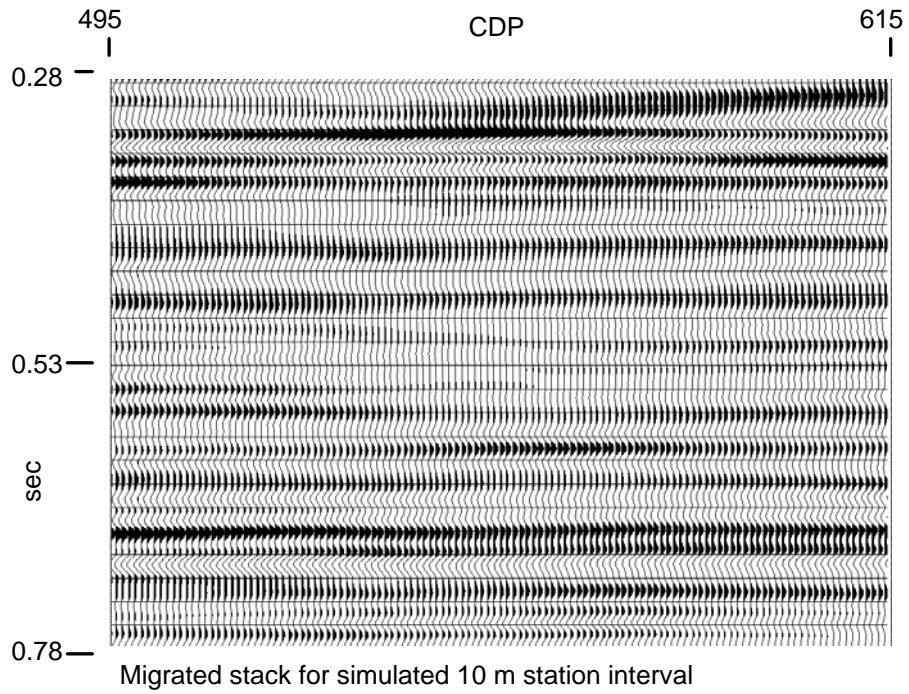


FIG. 42. Migrated stack image of 10 m data—view 3

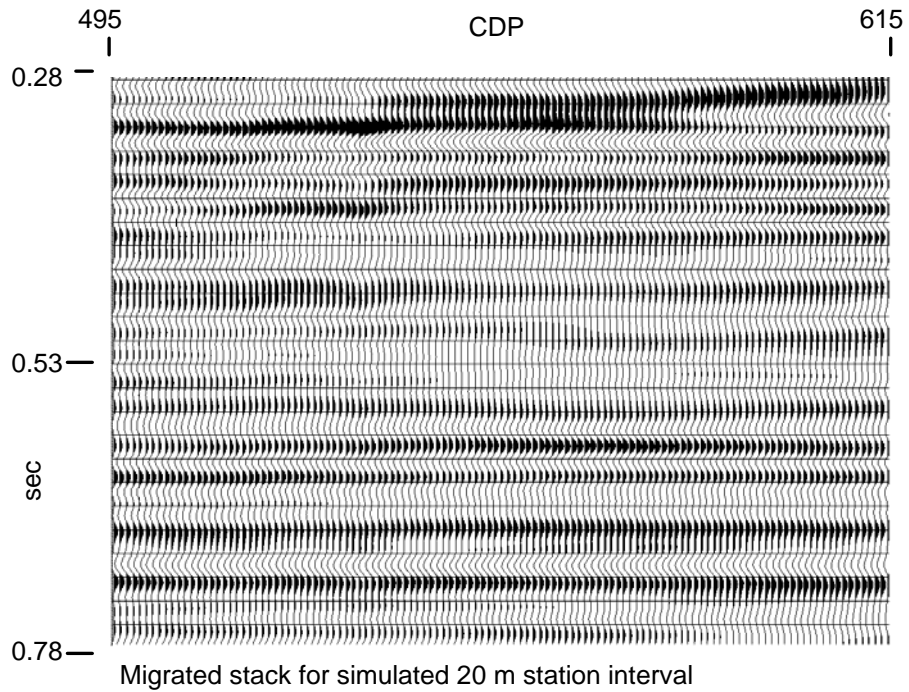


FIG. 43. Migrated stack image for 20 m data—view 3

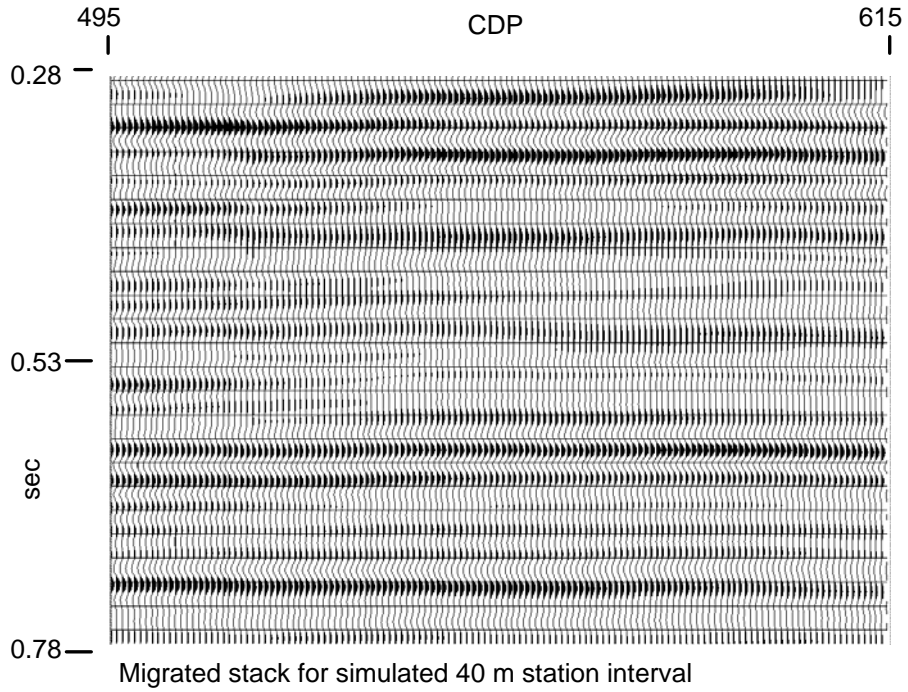


FIG. 44. Migrated stack image for 40 m data—view 3

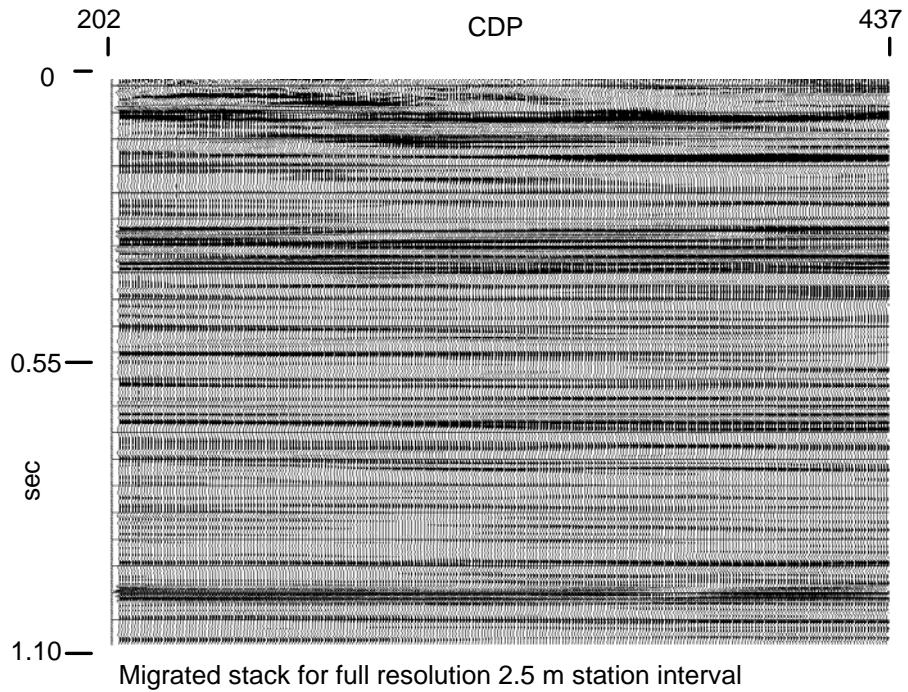


FIG. 45. Migrated stack image for 2.5 m data—view 4

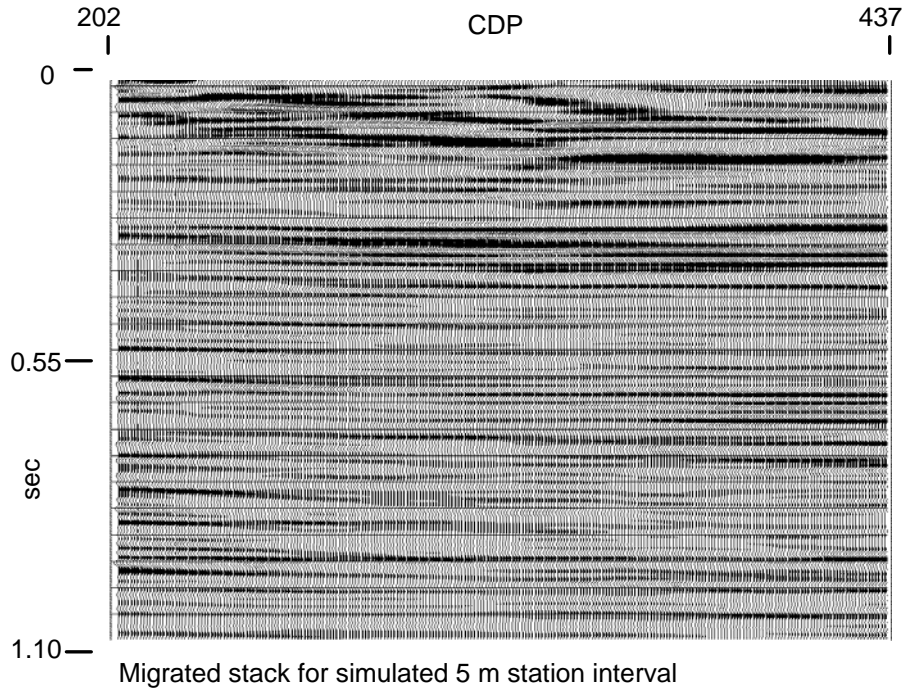


FIG. 46. Migrated stack image for 5 m data—view 4

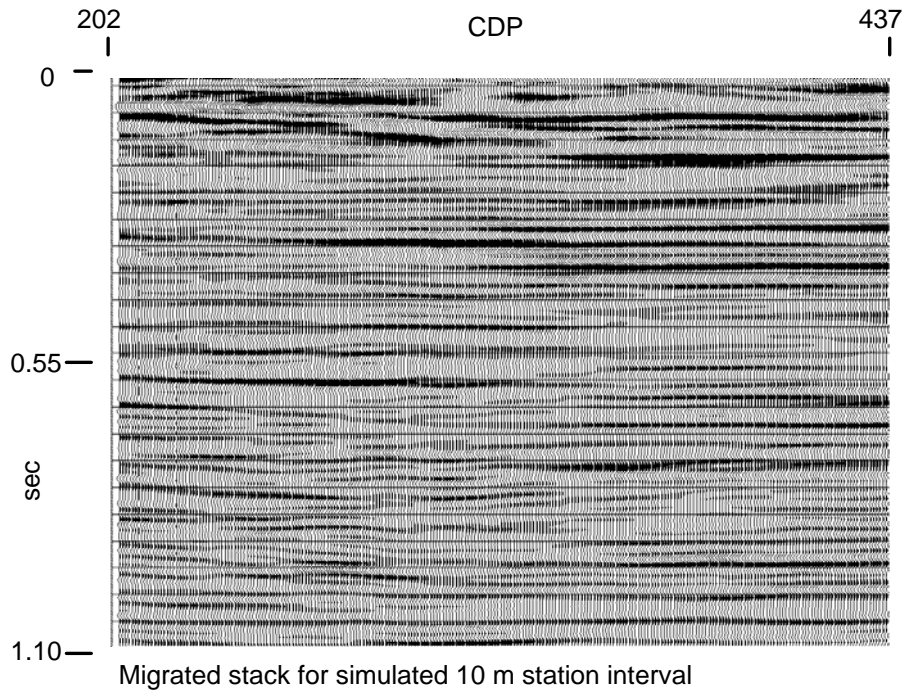


FIG. 47. Migrated stack image for 10 m data—view 4

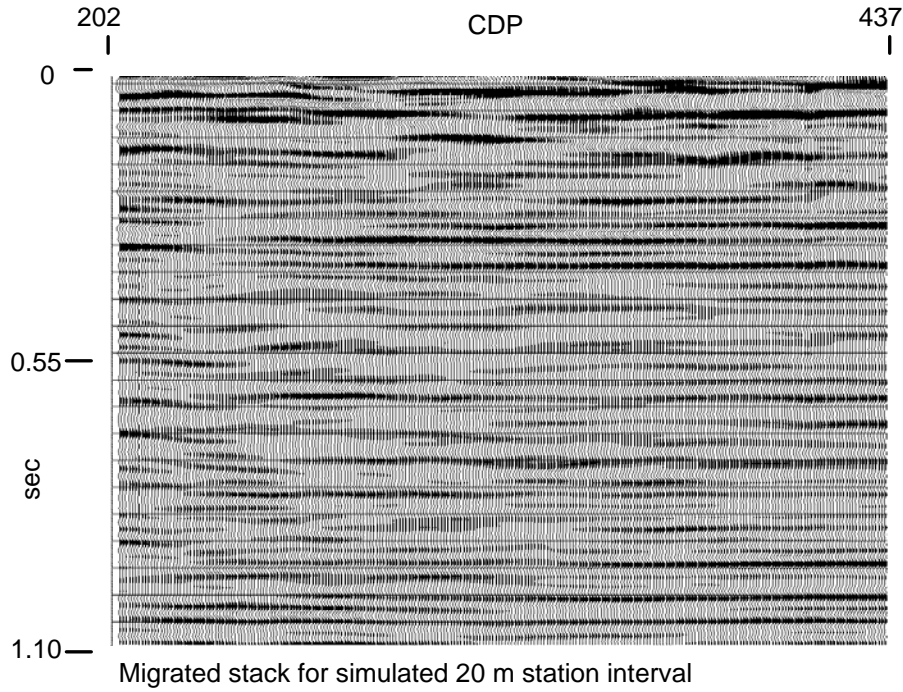


FIG. 48. Migrated stack image for 20 m data—view 4

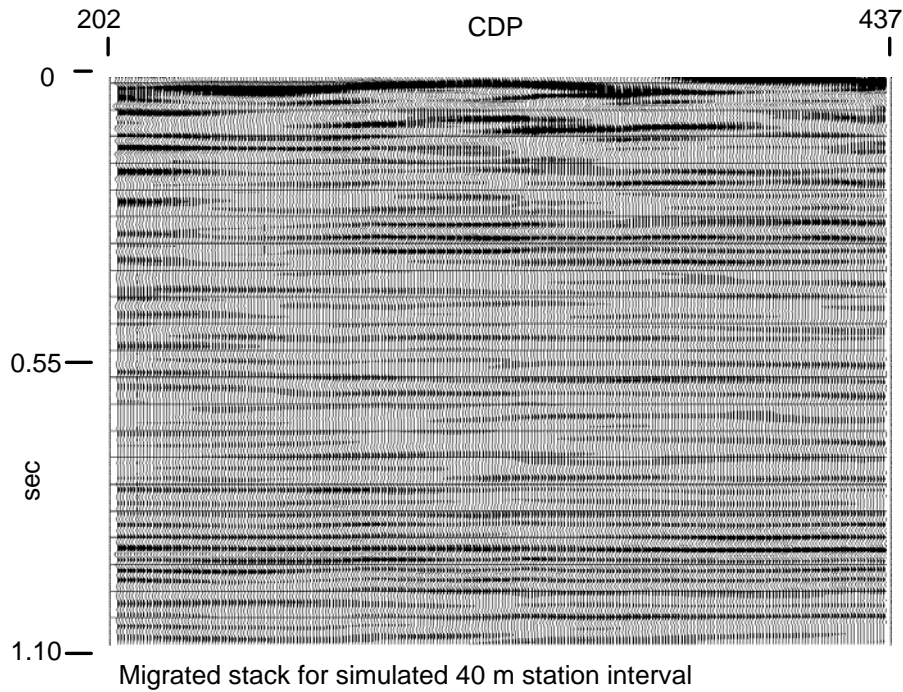


FIG. 49. Migrated stack image for 40 m data—view 4

CONCLUSIONS

The single strongest conclusion we can draw from this analysis is that, at least down to 2.5 m receiver spacing, recording with close-spaced single phones is superior to recording with the same phones wired in arrays, both in terms of lateral and vertical resolution. The surprise here is that detector spacing affects vertical resolution as well as lateral. A second conclusion is that no matter how hopelessly swamped with noise the shot gathers appear, if the noise is properly sampled, reflections may still be present and recoverable. The fact that we see reflections even on the 40 m data set is likely due to the extremely high fold of this simulated data set. If we had actually decimated the shot spacing, without array forming, to be comparable to the receiver spacing, rather than re-binning traces, we would almost certainly have more difficulty seeing coherent reflections.

For a given number of geophones, and a fixed geophone interval, it pays to record the phones individually rather than to hard-wire them into arrays, if sufficient recording channels are available. Decreasing the source interval comparably is also worthwhile, if the source is a vibrator and time is not an issue. With respect to acquisition time—our experience showed that seismic crew time might not be excessive even with our so-called “high-effort” approach. The 1 km survey described here required only about 10 hours to acquire with a crew of 8 relatively inexperienced University staff—about 3 hours to lay out and connect the 376 stations of single geophones, with careful attention to solid phone plants, about 2 hours to retrieve the phones, boxes and cables at the end of the day, and about 5 hours to vibrate the line with 4 10-second sweeps per station every 5 m along the line. Subsequent experience with the same equipment has shown, as well, that practice can reduce the time required for each phase of the acquisition.

ACKNOWLEDGEMENTS

The authors thank several staff members from CREWES for assistance during the acquisition of these data, including Zuolin Chen, Hanming Gu, and Joe Wong. In addition, we acknowledge the support of CREWES sponsors for this work.

REFERENCES

- Bertram, M.B., Lawton, D.C., Gallant, E.V., and Stewart, R.R., 2005, New seismic reflection and other geophysical equipment available to CREWES: CREWES 2005 research report, **17**.
- Henley, D.C., 2003a, Coherent noise attenuation in the radial trace domain, *Geophysics*, **68**, No. 4, (July-Aug 2003), pp1408-1416.
- Henley, D.C., 2003b, Deconvolution in the radial trace domain: CREWES 2003 research report, **15**.
- Henley, D.C., 2006, Ensemble-based deconvolution: when and why, CREWES 2006 research report, **18**.
- Hoffe, B.H., Margrave, G.F., Stewart, R.R., Foltinek, D.S., Bland, H.C., and Manning, P.M., 2002, Analyzing the effectiveness of receiver arrays for multicomponent seismic exploration: *Geophysics*, Vol. **67**, No. 6, (Nov-Dec 2002), pp1853-1868.